Using a Zebrafish Animal Model to Identify the First Candidate Gene for Pigmentary Glaucoma

By
Thien-Kim Nguyen-Phuoc

A thesis submitted in partial fulfillment for the degree of

Master of Science
Medical Sciences- Medical Genetics
University of Alberta

Abstract

Premelanosome protein (*PMEL*) was identified as a candidate gene for the development of pigment dispersion syndrome (PDS) and pigmentary glaucoma (PG) in humans. Mutations in PMEL were shown to cause pigment and ocular defects in several animals but there is currently no known PMEL associated defects in humans. We hypothesize that mutations in PMEL are associated with PG/PDS. To elucidate the pathology of PG/PDS, we analyzed the impact that mutations in a zebrafish homolog of PMEL (*pmela*) have on the structure and function of the zebrafish eye. Zebrafish are an excellent animal model for studying an ocular disease because of its genetic tractability and the zebrafish's similar ocular structure to the human eye.

We deployed morpholinos (MOs) and CRISPR/Cas9 to generate transient *pmela* knockdowns and *pmela* knockout zebrafish, respectively, to assess the requirement for PMEL in early development and ocular maintenance. We assayed ocular pigmentation, ocular structure, and anterior segment structure.

MOs targeted at a PMEL paralog in zebrafish (*pmela*) significantly reduced global pigmentation and ocular pigmentation. The disruption of *pmela* by CRISPR/Cas9 created two stable alleles. One allele, ua5022, when homozygous, caused significant global pigment reduction, enlarged anterior segments, microphthalmia, and a change in eye shape. The mRNA transcripts of *pmela* in the ua5022 homozygotes were reduced by 20-fold compared to wild type fish.

Using zebrafish as an animal model to ascertain the role of PMEL in the etiology of PG/PDS will help elucidate the mechanisms of the disease, leading to novel diagnosis and treatment avenues.

Preface

This thesis is an original work by Thien-Kim Nguyen-Phuoc in partial fulfillment towards a Master of Science at the University of Alberta.

Animal ethics approval was obtained from the University of Alberta Animal Care and Use Committee: Biosciences, protocol AUP00000077, under the auspices of the Canadian Council on Animal Care.

Portions of the abstract were modified from "Dissecting the Role of the Premelanosome Protein Gene (PMEL) in the Development of Pigmentary Glaucoma Using the Zebrafish Animal Model." Kim Nguyen-Phuoc *et al.* (2018). The Association for Research in Vision and Ophthalmology. May 2nd, 2018. Honolulu, USA. This abstract was submitted as part of a conference. I wrote the abstract and presented the poster. I performed the *in vivo* experiments associated with the research.

Portions of text and figures in Chapter 1 were modified from "Reduced Abundance and Subverted Functions of Proteins in Prion-Like Diseases: Gained Functions Fascinate but Lost Functions Affect Aetiology." Ted W. Allison *et al. (2017). Int. J. Mol. Sci.* 18(10), 2223. This work was a review done by the Allison lab to lend new insight into the investigation of prion diseases. I contributed through an analysis of functional amyloids and how mutations in such proteins can elucidate the disease mechanism of prion disease.

Portions of text and figures in Chapter 1, 2, 3, and 4 were modified from "Non-Synonymous variants in Premelanosome Protein (PMEL) cause ocular pigment dispersion and pigmentary glaucoma." Adrian A. Lahola-Chomiak *et al.* (Submitted). This work was a collaboration between Dr. W. Ted Allison's, Dr. Michael Walter's, and Dr. Ordan Lehmann's labs at the University of Alberta. Collaborations outside of the University of Alberta for this

work included Dr. Janey Wiggs' lab at the Massachusetts Eye and Ear Institute at Harvard Medical School, USA and Dr. Jamie Craig's lab from the Department Ophthalmology at the University of Flinders, Australia. The patients came from Dr. Ordan Lehman (CA, UK, US), Dr. Janey Wiggs (US), and Dr. Jamie Craig (AU). The genetic analysis was performed in the Walter lab (CA, UK, US), the Wiggs lab (US), and the Craig lab (AU). Adrian Lahola-Chomiak, of the Walter lab, did the *in vitro* studies of PMEL patient variants. I contributed to this by creating and analyzing the *in vivo* animal model.

To my supervisor, family, friends, and partner, I can't even begin to parse in a single phrase how much you have all made this experience for me.

"I hate to hear you talk about all women as if they were fine ladies instead of rational creatures. None of us want to be in calm waters all our lives."

"My idea of good company... is the company of clever, well-informed people, who have a great deal of conversation; that is what I call good company.'
'You are mistaken,' said he gently, 'that is not good company, that is the best."

Jane Austen, Persuasion

Acknowledgements

Thank you to everyone who has supported me while I completed my Master of Science here at the University of Alberta. From those who I have known from before coming here, to those that I met during my time here, I appreciate you all.

I would like to thank my supervisor W. Ted Allison. Ted, thank you very much for trusting me and supporting me during my time in your lab. I was a student who had only some background in genetics and couldn't stop talking about turtles, but you took me in and helped me learn. Because of you, I was able to get the experience out of my Master's that I wished for and for that I am grateful. Also thank you very much to my committee, Dr. Holger Wille and Dr. Michael Walter; your support and guidance during my Master's has also been immeasurable. Thank you do Dr. Jennifer Hocking for agreeing to be my external. I look forward to talking to you about my project! In addition, I would also like to thank Dr. Sarah Hughes and Dr. Rachel Wevrick who have kept me on track during my program and have always been available when I needed a helping hand. Lastly, thank you to the Medical Genetics Department admin team. I have bothered you a lot over the past 2.3 years and you have solved it all.

Thank you so much to all of the members of the Allison lab. Without all of you, my experience would not have been so fulfilling and rich. Phil and Michele, you two helped me be a better scientist and spent so much time making sure that I was on the right track. Gavin, thank you so much for helping me during my PMEL struggles. Hadeel, you have been a wonderful and uplifting presence in my life. I promise one day I will get to that list! Spencer, thank you so much for your support through out my project. Emily, thank you for always being such a strong and stable presence. Talking to you about science and life in general always grounded me, and in a Master's grounding was what I needed. And lastly, I would be remiss not to mention Nicole. We have been dubbed an old lesbian couple and yes, I am the biggest romantic threat. I have shared with you so many memories, lots of laughter, and tears, and precious to me, they are all. Also sorry for sneezing on you. Thank you so much for enriching my experience here in Edmonton.

I would like to express my gratitude to all of those in the Department of Medical Genetics. Adrian, you were the other half (two-thirds?) of the PMEL project. Thanks for reawakening the nerd/geek in me and loving food as much as I do. Alli, thank you for always being there. You were so supportive and talking to you always eased my worries. Lance, we bonded over a fire in the rain; thank you for all the laughter. I'm sorry I didn't get you cake that wouldn't kill you... twice. Tim, I am so grateful for all of your help with my project. You were patient and kind in guiding me through things I didn't understand and helped me solve so many of my problems. Also, thank you for the board game lunches and dinners, and introducing me to your dogs. They are the best dogs. And to Matthea, thank you for the crazy nights out, the "patio" beers, the drunken escape rooms, and the tea. Jasper is a crazy dog, and you tricked him into accepting pets from me.

There are so many others that I have met during my Master's, who if I named dropped, this list would go on longer than my introduction, but you have all been a part of my wonderful experience here. However, I do need to mention two people in particular. Thank you so much Shima. You have been a wonderful friend who has supported me since the very beginning of my Master's. You dragged me into a black hole of which I have not been able to escape and for some reason maybe don't want to escape? and it has caused

chaos in my life every since. In that black hole, the person who has been by my side through thick and thin has been Zhao. I shared with you some of the most stressful, non-academic moments of my degree and we survived it together two years in a row. We can survive the third. Thank you so much for being such an amazing colleague and from that we have developed such a supportive friendship. I hope that we will have the chance to work together again someday.

To all of my friends back home who I have shared a better portion of my life. Some of you I have known for two decades, others as recently as one decade. You all have been there for me during my best and during my worst. I would not be who I am today without all of you. If I could be considered a good person, it is only because you have all made me better. Vivian, our star-crossed friendship is only going to get more star-crossed from here on out, but no matter the distance between us, I know that you'll always be there for me. We are still the best couple. Cindy, your unwavering support and companionship is priceless. You have stood by me in situation where I couldn't stand for myself and are always there to lend an ear. I hope that I have been the same for you. Jen, when we talk we talk about the depths of reality. The easy and the hard, I can always explore with you. Michelle, there is so much to say about our relationship. It is most certainly the most dynamic and crazy. I wouldn't trade it for the world. Kevin, our friendship has gone through ups and downs, but it's only made it stronger. Thank you for being a nuisance when I need the distraction and being there when ever I needed a helping hand or voice. I do blame you for the 20,000 words that weren't for my thesis.

My mother. Thank you so much for your love and support. You gave me a life where I could have every opportunity and taught me how to persevere through the good times and the bad. You gave me my appreciation for food and travel, both of which I cherish one could say, too much. I am grateful to my sister, who being much older than me, has always had wise words and has been an incredible source of guidance in my life. You have always challenged me to be a better person. Thank you to my father who has been there when I needed him most. To my nan, I hope that you are happy. To the James family, who welcomed me with open arms when I was, on incredibly short notice, thrown into your household and have stuck around ever since. Nick, Kath, Gwen, and Megan, I am so grateful for your love and warmth. I will continue to try, but I don't think I'll ever be able to top the inflatable turkey. Thank you for your unwavering encouragement.

And lastly, but most importantly, Huw. Words cannot describe the depth of my appreciation in having you in my life, but let me try. We met under the most unlikely of circumstances and have lived an ocean apart ever since. Despite the distance and the years, we have persevered. Being with you has made me a better person. You have loved me through my best and have loved, accepted and most of all, tolerated me at my worst. I'm sorry I have a tendency to disappear on nights out; at least you can usually find me at the local McDonald's. We have shared so many adventures together and I hope that we will continue to share many more. I am so excited for the next chapter in our lives together. Thank you so much for loving me. Rydw i'n caru ti.

Table of Contents

List of Tables

List of Figures

List of Abbreviations

APP	amyloid beta precursor protein
AU	Australia
CA	Canada
CAF	core amyloid fragment
CRISPR	clustered regularly interspaced short palindromic repeats
CYT	cytoplasmic region
dpf	days post fertilization
IDT	Integrated DNA Technologies
KLD	Kringle-like domain
MO	morpholino
NEB	New England Biolabs
NHEJ	non-homologous end joining
NTR	N-terminal domain
PAM	protospacer adjacent motif
PDS	pigment dispersion syndrome
PG	pigmentary glaucoma
PKD	polycystic kidney-like domain
RGC	retinal ganglion cell
PCR	polymerase chain reaction
PMEL	premelanosome protein
RPE	retinal pigment epithelium
RPT	repeat region
SP	signal peptide
TALEN	transcription activator-like effector nuclease
TM	transmembrane domain
UK	United Kingdom
US	United States
WES	whole exome sequences
ZFN	zinc finger nuclease

Chapter 1: Introduction

1.1 The Eye

The eye is the sensory organ that gives us our sense of sight. It is highly organized, creating a succinct pathway for light signals to be captured and transmitted to the brain. In humans, the majority of eye development occurs between week three and week eight of development[1, 2]. The eye is part of our central nervous system, deriving from the brain/neural tube[2]. The eye is composed of neural ectoderm, surface ectoderm, and mesoderm[2, 3]. The neural ectoderm, which is the tissue derived from the brain/neural tube, forms structures such as the retina, the retinal pigment epithelium (RPE), the iris, and the ciliary body. When the neural ectoderm comes into contact with the surface ectoderm, part of the surface ectoderm invaginates and forms the lens, while some of the surface ectoderm forms the epithelium of the cornea. The mesoderm forms the rest of the cornea, the trabecular meshwork, and the sclera of the eye[2, 3].

The eye can be separated into two segments: the anterior segment and the posterior segment (Figure 1). The anterior segment of the eye contains both the anterior chamber and the posterior chamber of the eye, which encapsulate structures such as the cornea, trabecular meshwork, iris, ciliary body, and lens. The anterior segment contains the aqueous humor. Structures of the anterior segment of the eye, ie. the cornea and lens, are responsible for the focusing of light on the macula of the retina. The cornea cannot be adjusted for focus; however, the ciliary body can alter the shape of the lens through structures called zonules in order to change the focus of light on the retina. The iris is a muscle that controls the size of the pupil to change how much light can enter the eye. The posterior segment of the eye contains the vitreous chamber, the retina, and the choroid. The vitreous chamber contains vitreous humor, which maintains the shape of the eye. The

choroid is the vascular layer of the eye, providing the eye with oxygen along with the retinal artery [4].

Fluid pressure in the eye is maintained through the production of aqueous humor, which is produced circumferentially in the ciliary body in the posterior chamber of the anterior segment. Fluid circulation in the eye will then bring the aqueous humor from the posterior chamber into the center of the anterior chamber of the eye, through the pupil, before draining circumferentially through the trabecular meshwork and out of the eye via Schlemm's canal and the uveoscleral pathway[5].
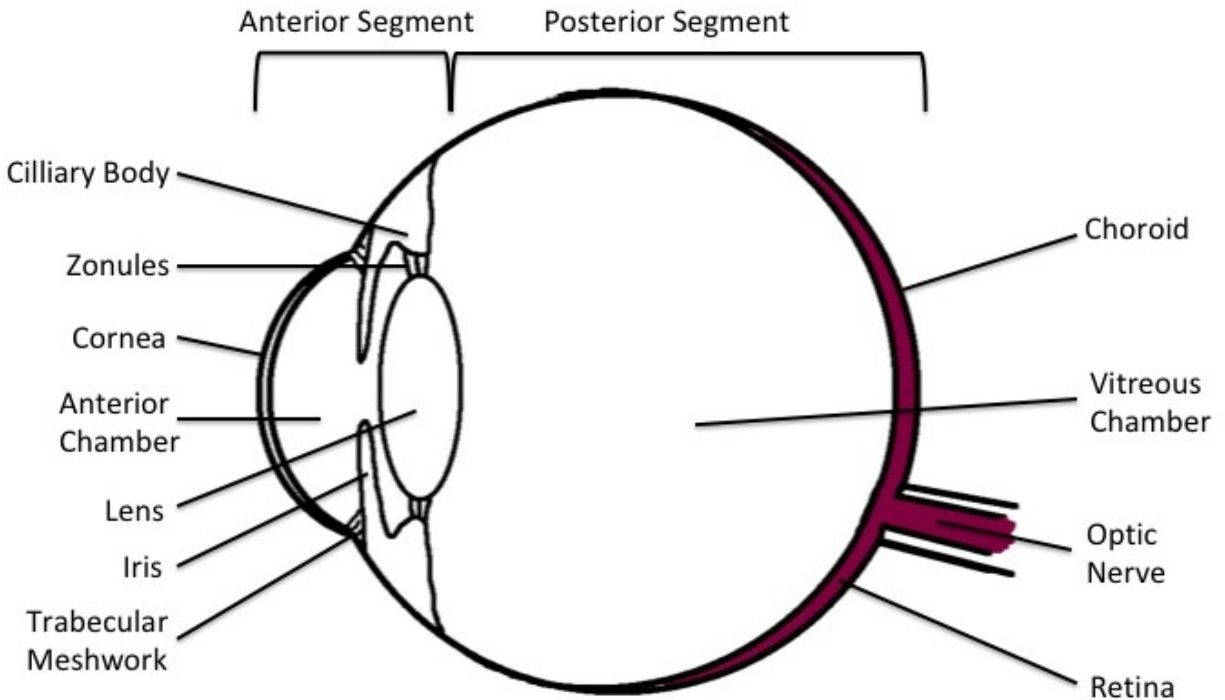
Figure 1: The human eye divided into the anterior and posterior segments.
The anterior segment of the eye is composed of the anterior chamber and the posterior chamber and contains the aqueous humour. Structures found in the anterior segment of the eye include: the cilliary body, the zonules, the cornea, the anterior chamber, the lens, the iris, and the trabecular meshwork. The posterior segment of the eye is composed of the vitreous chamber, the retina, and the choroid. The optic nerve projects out of the posterior segment and connects the signals of the eye to the brain.

The retina is a highly organized sensory layer of cells that detects light and transmits the captured signals to our brain so that we are able to interpret visual information. The cells that detect the light are called photoreceptors, of which there are two types, rods and cones. Rods are photoreceptors that are extremely sensitive to light and allow for us to see in dim light settings, but do not allow us to see in colour. Meanwhile, cones are the photoreceptors that allow us to see in colour, but are not nearly as sensitive as rods. The outer segments of the photoreceptors are turned over in the retina by the retinal pigment epithelium (RPE)[6]. The cells that transmit visual information from the eye to the brain are called the retinal ganglion cells (RGCs). The axons of RGCs form the optic nerve, which is the highway upon which the visual information travels out of the eye and into the brain to synapse at the superior colliculus or the geniculate nucleus, where that visual signal will then travel to the visual cortex [7]. The point at which the axons of the RGCs, the optic nerve, exits the eye is called the optic disc. The orientation of the retina is so that the RGCs are closest to the center of the eye, while the photoreceptors are on the outer edge with their outer segments oriented away from the anterior segment of the eye (Figure 2).

Pigmented structures in the eye include the posterior side of the iris, the RPE, and the choroid. Of these pigmented structures only one is in the anterior segment of the eye, the iris. The disruption of pigmented cells can lead to diseases, such as pigment dispersion syndrome and pigmentary glaucoma.
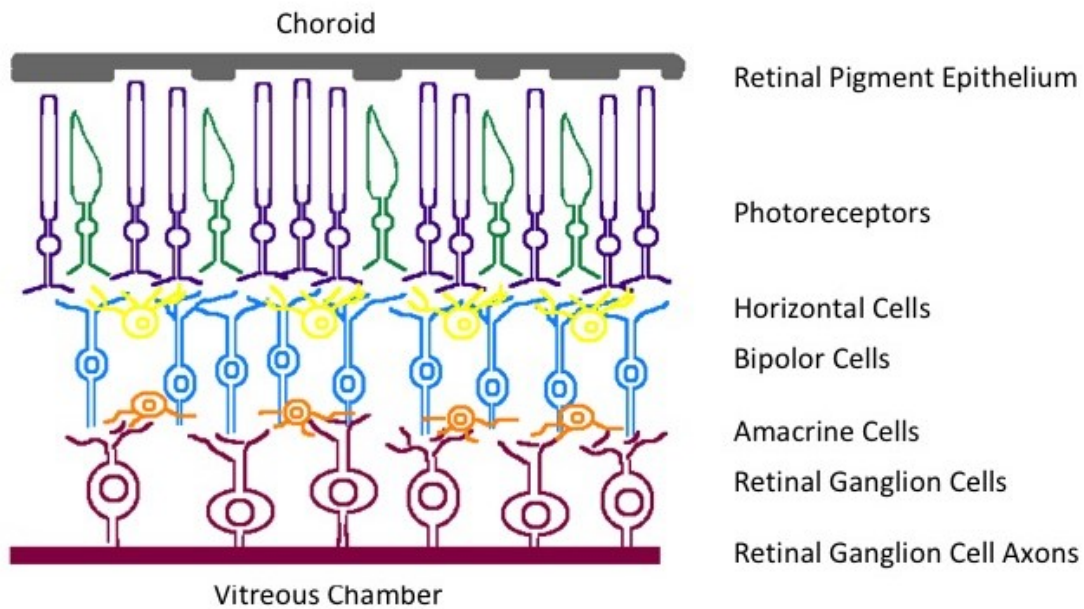
Figure 2: The retina of the human eye.
The retina of the eye is composed of several cell types including the retinal pigment epithelium, the photoreceptors, the horizontal cells, the bipolar cells, the amacrine cells, and the retinal ganglion cells. The axons of the retinal ganglion cells gather on the inner most layer of the retina and exit the eye via the optic nerve (Figure 1) to transmit signals to the brain.

1.2 Pigmentary Glaucoma and Pigment Dispersion Syndrome

Glaucoma is the leading cause of irreversible, non-traumatic blindness with over 3.5% of people affected worldwide[8-11]. The defining attribute of glaucoma is the death of RGCs, which disrupts the transmission of signals from the retina to the brain [9, 11-15]. Glaucoma is a highly heterogeneous disease with many genetic and environmental factors involved in its development[9-11, 15, 16].

There are two major forms of glaucoma, open angle and closed angle[9, 10, 15, 17]. Primary closed angle glaucoma is characterized by the closure of the iridocorneal angle, preventing the outflow of aqueous humor. Primary closed angle glaucoma is most prevalent in Asian populations[8-10, 18]. Open angle glaucoma is much more common and is characterized by the lack of closure at the iridocorneal angle[9, 17, 19]. Furthermore, open angle glaucoma can be sub-typed into primary and secondary glaucoma types[9, 10]. In primary glaucoma subtypes, there is no detectable resistance to aqueous humor outflow, while in secondary glaucoma subtypes there is a noticeable obstruction. Primary open angle glaucoma is most prevalent in African populations[8, 17, 20].

Glaucoma is highly associated with high intraocular pressure. High intraocular pressure is often used to diagnose glaucoma. However, it is possible to have glaucoma without high intraocular pressure and to have high intraocular pressure without glaucoma[9, 12, 17, 21, 22]. High intraocular pressure is closely associated with glaucoma because the pressure puts more force on the optic nerve head than the optic nerve head can withstand[12, 23]. Other risk factors that are associated with glaucoma include age, ethnicity, family history, and myopia[9].

The most common secondary glaucoma subtype is pigmentary glaucoma (PG). The prevalence of PG has an extremely large range: 0.0014% to 2.45% of the population are estimated to be affected in the United States[24-30].

PG is defined by the diagnosis of pigment dispersion syndrome (PDS) and the characteristic rise in intraocular pressure common to many glaucoma subtypes[24, 31]. PDS is the abnormal sloughing of pigment from the posterior side of the iris. PDS does not impair vision but is a major risk factor for the development of PG[24, 25, 31, 32]. Recently, it has been theorized that the pigment granules in PDS do not originate from the iris alone, but also the RPE. The pigment circulates in the anterior chamber of the eye where it can deposit on the cornea in the form of a structure called the Krukenburg spindle (Figure 3a), and/or deposit in the trabecular meshwork (Figure 3c)[24, 26, 31-33]. Another symptom of PDS is the aberrant passage of light through the iris, termed iris transillumination, due to a loss of pigmented cells (Figure 3b) [24-26, 32, 33]. The estimation of those affected is so highly ranged and convoluted by the challenges in the diagnosis of the disease. The physical symptoms of PDS are often transient and subclinical, making the diagnosis of PDS, and therefore the diagnosis of PG, challenging. The transient and subclinical nature of PDS is a major factor in the large range of pigmentary glaucoma prevalence in the United States.
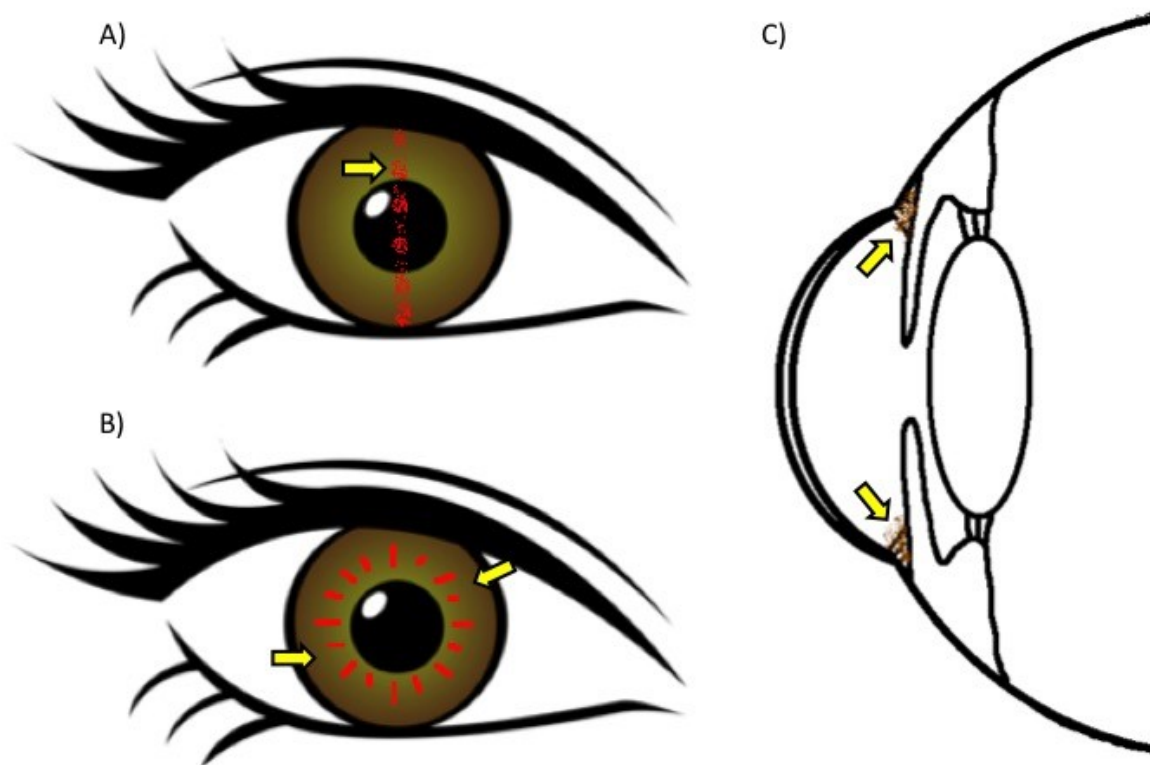
Figure 3: Indications of pigment dispersion syndrome.
A) *Krukenburg spindle. Due to the circulation of the aqueous humour in the anterior segment of the eye, pigment can deposit in a vertical line on the cornea.* *B)* *Iris transillumination. Normally when light is shone into the pupil and reflects off of the back of the eye, the light will only be able to reflect back out of the pupil due to pigment blocking the passage of light through the iris. However, if there is iris transillumination, the reflected light can also be seen shining back through holes in the iris. The holes in the iris are often circumferential.* *C)* *Pigment deposition in the trabecular meshwork. Due to the outflow of aqueous humour through the trabecular meshwork, pigment granules that are not otherwise deposited elsewhere (such as on the cornea) deposit in the trabecular meshwork where the pigment can be observed.*

Currently, the pathology of PG is unknown. Although PDS is present in those with PG, the relationship and causality between the two conditions also remains cryptic[24, 28]. Historically, there have been two schools of thought when it comes to the mechanism of pigment sloughing in PG/PDS: structural and dysfunctional[24]. The structural school of thought believes that it is the rubbing of the zonules against the iris that causes the shedding of pigment[24-26, 34]. This theory is supported by the observation of several patients with PG/PDS who have zonules that are bowed abnormally, allowing for contact with the iris[24, 25]. The dysfunctional school of thought theorizes that a genetic mutation causes cell death leading to the shedding of pigment cells from the iris[24, 26]. This school of thought is supported by the observation of abnormal pigmentation development on the posterior side of the iris[35] and that in certain populations of PG/PDS patients, structural contacts between the zonules and the iris are less abundant[36]. Animal models of PG/PDS also provide support for the dysfunctional school of thought, in that this disease is usually best replicated by mutations that affect proper synthesis of iris pigment rather than the structure of the zonules[24]. Recently, these two schools of thought have been combined into a theory proposing a genetic predisposition to the dysfunction of the pigmented cells of the iris that is exacerbated by mechanically induced release of pigment by bowed zonules[26]. Current models and hypotheses have not successfully led to the development of effective non-palliative treatments for patients. It is vital that we better understand the mechanisms of PG's development, as it is a major cause of blindness globally[8].

Current research heavily supports a genetic basis for PG: 26 to 28% of PG patients report a family history of glaucoma, and several loci have been mapped in family

studies[26, 31]. Despite this progress, to date, no candidate genes have been identified for PG in humans.

1.3 Identifying Candidate Genes via Whole Exome Sequencing

To find genes that are associated with PG/PDS, whole exome sequencing (WES) was performed by our collaborators (Walter lab) on individuals from two families with a history of PG from North America. Genes that were highly associated with PG/PDS in these families were then targeted for sequencing in a panel of 113 sporadic cases of patients from Canada (CA) and the United Kingdom (UK) with PG. Several candidate genes were identified through this method; the most promising of which was premelanosome protein (*PMEL*)[37].

Independently, *PMEL* was also determined to be a candidate gene for PG/PDS when WES was performed in an American family with a history of PG and then targeted for sequencing in panel of 146 sporadic cases consisting of patients from the United States of America (US) (Wiggs lab). The findings from the two labs were then further verified by targeted sequencing in an Australian cohort (AU) of 135 sporadic cases of PG (Craig lab)[37].

1.4 Premelanosome Protein

PMEL is a type I transmembrane glycoprotein found in melanosomes, pigmented organelles that are found in pigmented cells called melanocytes[38, 39]. PMEL is also known as Pmel17, gp100, Silver, SILV, and ME20[39]. Particular domains of the processed protein act as the fibril scaffold for melanin synthesis while the other domains aid in the proper processing of PMEL[38, 39]. There are two different types of melanin that give rise to different pigments: eumelanin, which produces black/brown pigment and pheomelanin, which produces red/yellow pigment[38]. In melanosomes, eumelanin is more common[39]. Proper processing of PMEL is thought to be additionally important for the removal of toxic intermediates that build up during the synthesis of melanin[39, 40].

PMEL is composed of the signal peptide (SP) and seven different domains: the N-terminal region (NTR), the core amyloid fragment (CAF), the polycystic kidney-like domain (PKD), the repeat region (RPT), the Kringle-like domain (KLD), the transmembrane domain (TM), and the cytoplasmic region (CYT) (Figure 4). PMEL is synthesized in the endoplasmic reticulum and is heavily processed in several steps that take place in the endoplasmic reticulum, the Golgi apparatus, and in endosomal compartments, which eventually become melanosomes[38, 39].
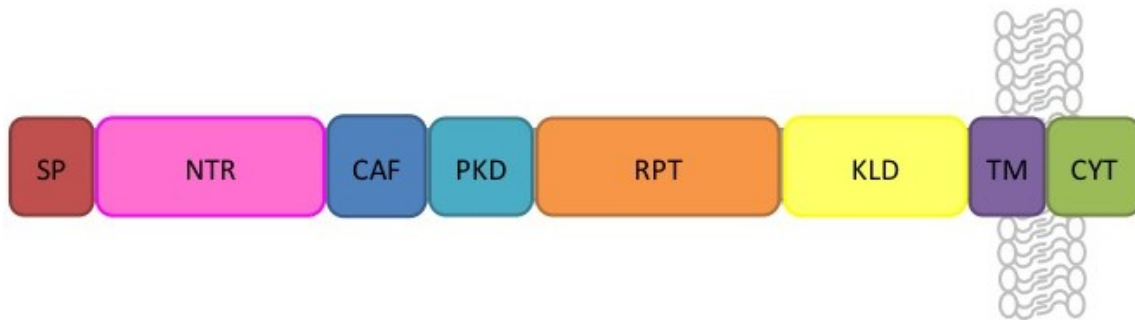
Figure 4: The domains of premelanosome protein (PMEL).
Signal peptide (SP), N-terminal region (NTR), core amyloid fragment (CAF), polycystic kidney-like domain (PKD), repeat region (RPT), Kringle-like domain (KLD), transmembrane domain (TM), and cytoplasmic domain (CYT). The NTR and the KLD have sites of N-linked glycosylation while the RPT has many sites of O-linked glycosylation.

Table 1: Mutations in PMEL Found in Individuals with PDS/PG

Mutation	Cohort	Domain
p.N111S	CA/UK	N-Terminal Region
p.G175S	US Family 3	Core Amyloid Fragment
p.G325V	US	Repeat Region
p.V332I	AU	Repeat Region
p.A340V	CA Family 1	Repeat Region
p.E370D	CA/UK/AU	Repeat Region
p.S371T	AU	Repeat Region
p.L389P	CA/UK/US	Repeat Region
p.Δ641-642	US	Cytoplasmic Domain

The NTR is described to be important in the proper processing of the fibril scaffold in the melanosome, in particular the proper processing of the PKD. When the NTR is deleted, the fibrillar scaffold does not form[41]. Through the use of single amino acid mutations, only certain residues in the NTR were found to be crucial for processing[42]; our patient variant in the NTR not being one of them.

The CAF is the most recently characterized domain in PMEL. The CAF is a segment of the processed protein that composes the fibril matrix in melanosomes upon which melanin is synthesized. The CAF was investigated as being part of the fibril structure of melanosomes due to some *in vitro* studies demonstrating that fibrils can form in the absence of the RPT[43, 44].

The PKD and the RPT are regions in PMEL that have long been characterized to be a part of the protein structure of the fibrils in melanosomes. The deletion of the PKD, similar to the NTR, results in the lack of fibril formation[41]. PMEL lacking the RPT create circular, disorganized looking melanosomes that lack fibrils[41, 45]. It has also been found that *in vitro* fibrils can form from just the RPT sequence alone[46, 47]. The fibrils that are formed by the RPT can only form and retain their fibril structure under acidic conditions and will not form or dissolve under basic conditions[46, 47]. The early conditions of melanosomes are acidic in nature, supporting the role of the RPT in the fibril structure of melanosomes; however, the condition of the melanosome does not remain acidic[38, 48]. Due to these properties of the melanosome, it is theorized that the RPT cannot be the only domain of PMEL that constitutes the fibril structure of the melanosomes[43, 44].

The KLD was characterized to be important in the proper processing of the PMEL protein due to its proximity to a disulfide bond. The disulfide bond keeps the KLD and the

RPT attached even after the cleavage between the two domains in the Golgi apparatus until the disulfide bond breaks and the domains separate in the early endosome stage[49].

The TM is the region by which the protein is anchored to the membrane in the endoplasmic reticulum, Golgi apparatus, and endosome, until the protein is fully processed. It has been found that mutating this region can alter the PMEL amyloid protein from functional to pathogenic. The conversion is speculated to be due to the aberrant accumulation of fibrils in the melanosomes[50].

Mutations in the CYT seem to affect the proper trafficking of PMEL into the endosomes resulting in the decrease of protein and eventually the inability to form fibrils[51]. Mutations that could be categorized as in the CYT of many animals are often considered to be in the TM[50].

The stages of melanosome formation can be characterized by the appearance of PMEL fibrils (Figure 5). In stage 1, the fibril structure composed of the CAF, PKD, and RPT of PMEL cannot be observed although they are in the compartment. In stage 2, the fibril structure is apparent, but melanin synthesis has not yet been initiated. Melanin synthesis characterizes stage 3 melanosomes where both pigment and fibril structure can both be observed and stage 4 melanosomes have enough pigment production that the fibril structure of PMEL can no longer be seen[38, 39].
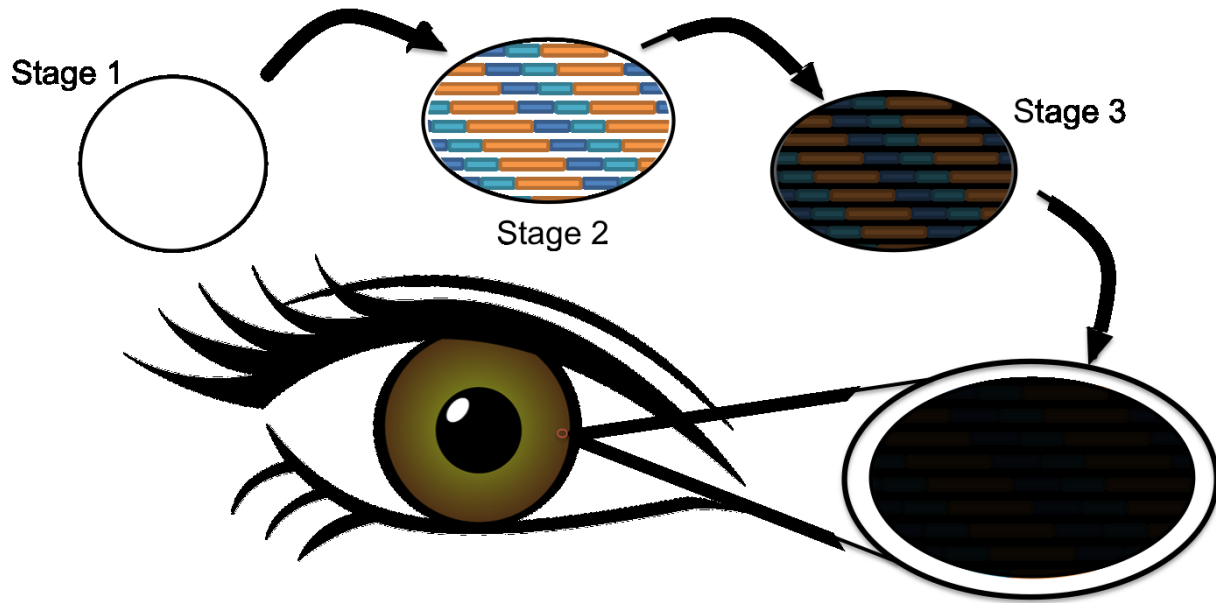
Figure 5: PMEL's role in melanosome development[52].
PMEL and the fibril structure that is created by the core amyloid fragment (CAF), the polycystic kidney-like domain (PKD), and the repeat region (RPT) are integral in defining the stages of melanosome development. At stage 1, there are no observable fibrils. This stage is can also be classified as the early endosome phase. At stage 2, the fibril structure formed by the CAF, PKD, and RPT are visible, but melanin has not begun synthesis. The shape of the melanosome changes from spherical to ovular due to the extension of the fibrils in the melanosome compartment. At stage 3, melanin begins to synthesize but the fibrils are still visible. At stage 4 enough melanin has been synthesized that the fibrils are no longer observable.

1.5 Functional vs. Pathogenic Amyloids

PMEL is a unique protein, for it is one of few known functional amyloids that have been identified in vertebrates and is the only functional amyloid to be identified as such consistently through out the literature[38-40, 53]. Although the literature is inconsistent in terms of which other amyloids are considered "functional", fibrin and RIP1/RIP3 are commonly listed amyloids [40, 54]. Amyloids are stable, insoluble protein structures composed mostly of β-sheets[55]. Amyloids are historically characterized as pathogenic, and contributions to diseases such as Alzheimers, Parkinsons, and Huntingtons[40, 53]. Amyloids are also implicated in prion diseases such as transmissible spongiform encephalopathy (mad cow disease) and fatal familial insomnia[56, 57]. However, the existence of PMEL as a functional amyloid disproves that the amyloid structure is inherently pathogenic[40, 53].

Understanding the proper function of PMEL and how mutations in PMEL can cause disease may also help elucidate the role of the amyloid proteins in the aforementioned diseases. In addition, understanding how the cell isolates PMEL to prevent toxic effects from the amyloid can help us control the toxic effects of pathogenic amyloids. The mechanisms that control PMEL include the tight regulation of PMEL formation, the compartmentalization of PMEL products in endosomes, and the quick kinetics of PMEL aggregation, especially when compared to the kinetics of other amyloids[38]. There is also a potential of pH regulation of fibril formation[47, 48]. Through studying how PMEL associates with glaucoma, a disease of the central nervous system, we can gain more insight into how other amyloids cause other nervous system diseases.

In addition, PMEL is processed similarly to how amyloid beta precursor protein (APP) is processed to Aβ-42 in Alzheimers disease(Figure 6). Both proteins are cleaved by related β-secretases on the N-terminus of the their transmembrane domain, APP with β-secretase 1 (BACE1) and PMEL with β-secretase 2 (BACE2) and then both are cleaved by a γ-secretase at the C-terminus of the transmembrane domain[58]. Although the function of the fragment produced in PMEL is currently unknown, the investigation of the role of this fragment in PG/PDS may provide some answers. This similarity could be used to better understand how pathogenic amyloids are made.
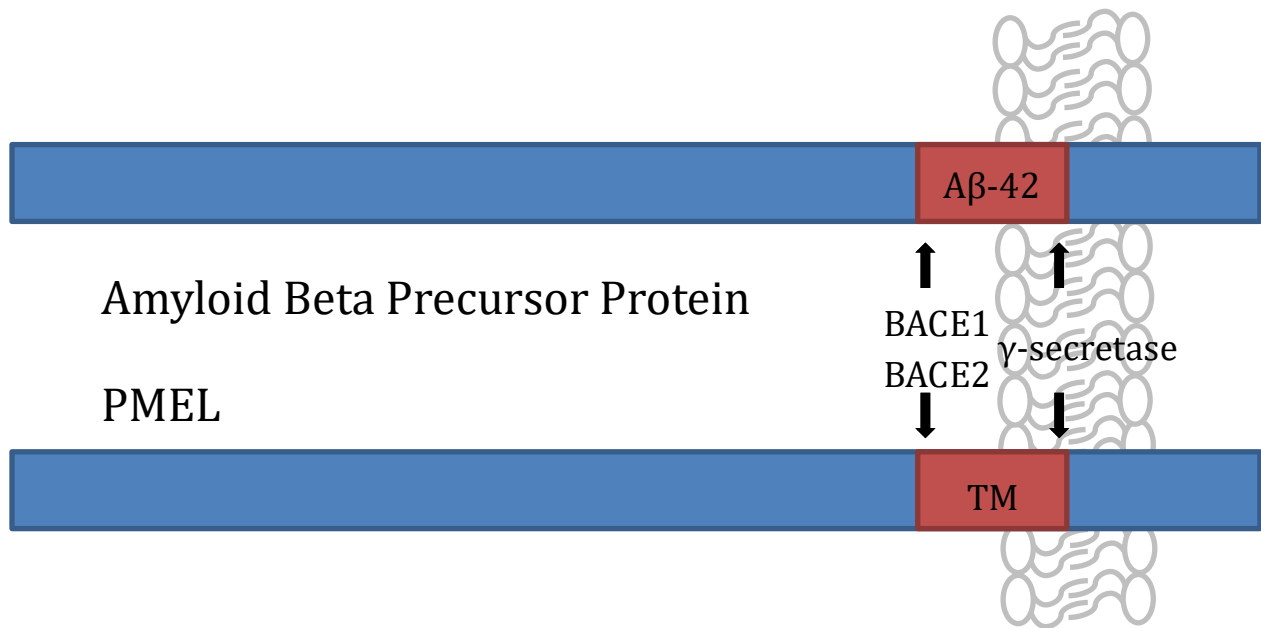
Figure 6: The processing of amyloid beta precusor protein to Aβ-42 is similar to the processing of the transmembrane domain (TM) of PMEL.
Both proteins are cleaved by related β-secretases, BACE1 and BACE2, and γ-secretases. Although both are amyloids and are processed similarly, Aβ-42 is pathogenic while the proper processing of the PMEL TM creates a functional amyloid.

1.6 Mutant PMEL in Animals

Although mutations in PMEL have not yet been associated with human disease, mutations in PMEL and their effect are well known in the animal world. Colouration changes due to mutations in PMEL have been found in cattle[59-61], horses[62], dogs[63], mice[64, 65], chickens[66], and zebrafish[67]. Interestingly, when more closely observed, the same PMEL mutation that is associated with the differential colouration in horses[68], dogs[63], mice[64], chickens[69], and zebrafish[67, 70] are also associated with a range of different abnormal ocular phenotypes.

Figure 7: Mutations found in PMEL homologs in animals with colouration mutations.
Note*: The loctions of all seven domains in the PMEL homologs have not been identified and therefore are not represented in this schematic, although the domains are well conserved across species. The gray bar represented the amino acids sequence with no definitive domain associated.
__A)__ Cattle. There are three PMEL mutations. Only the two mutations in the signal peptide (SP) are associated directly with changes in colouration. __B)__ Horses. Only one mutation in horses was identified in the transmembrane domain (TM)/cytoplasmic domain (CYT). The mutation is associated with both the silver dapple coat colouration and with the equinine multiple congenital ocular anomalies associated with the silver dapple coat colour. __C)__ Canines. There is one known mutation in canines, an insertion of a retrotransposon in the TM/CYT. The mutation is responsible for the merle coat colour. The mutation was found to be causative of the multiple congenital ocular anomalies found in merle dogs. __D)__ Mice. In the sequencing of silver mice, five mutations in PMEL were found, four of which were missense mutations. The last mutation, an insertion causing a frameshift in the TM, was theorized to be the causative mutation of the silver coat colour due to its similar location in the gene to causative mutations found in the silver dapple horses and dominant white chickens. __E)__ Chickens. Mutations in PMEL are found in many different chicken colourations, but only three morphs of chicken plumage are caused by mutations in PMEL. The dominant white plumage is caused by a three amino acid insertion in the TM, the smoky *plumage is caused by an additional four amino acid deletion in the PKD, and the dun plumage is thought to be caused by a five amino acid deletion in the TM. The five amino acid deletion in the TM is implicated due to its placement in the PMEL protein although there were many other missense mutations in PMEL associated to dun. __F)__ Zebrafish. The causative mutation in fading vision zebrafish is a nonsense mutation in pmela, one of two PMEL paralogs in zebrafish. This mutation is associated with reduced vision and global reduction in pigmentation.*

1.6.1 Cattle

In different pigmentation studies of cattle, *PMEL* was identified as a gene that is associated with changes in cattle coat colour [59, 61]. The two genes were found to work in concert in order to produce many different coat colours ranging from black to off-white[61].

The identified mutations in PMEL include a one amino acid, L, deletion in the SP, Δ18[59-61]; a missense mutation in the SP, G22R[59-61]; and a missense mutation in the CYT that has been noted as either A610E or A612E depending on the source (Figure 7a)[59, 61]. The amino acid deletion in the SP causes a dilute coat colour and is also causative of rat-tail syndrome[59]. Although the G22R missense mutation was associated with several different coat colours, it was found not to be responsible for the whole range of different coat colours[60]. The missense mutation in the CYT, although found in many cattle with pigmentation defects, has currently not been found to be causative of any changes in pigmentation[59, 61].

1.6.2 Horses

A single mutation in PMEL was independently found to be causative of the silver dapple coat phenotype and cases of equine multiple congenital ocular anomalies in horses[62, 68]. The silver dapple phenotype is the dilution and mottling of coat colour which is seen only in the body, and not the tail or the mane [62]. The PMEL mutation found in silver dapple horses is a missense mutation resulting in the conversation of R to C at amino acid 625[68] (or 618 in older literature[62]) in the CYT (Figure 7b).

1.6.3 Canines

PMEL is the gene responsible for an often sought-after coat colour, merle, in dogs. The insertion of a retrotransposon in the TM and the CYT in just one copy of *PMEL* causes this mottled coat colour. Heterozygous merle dogs have some ocular deformities such as microophthalmia (small eyes) and coloboma (a hole in a structure of the eye). Homozygous mutants, or double merle, dogs have nearly no global pigment, severe, often lethal, abnormalities, and severe ocular anomalies (Figure 7c)[63].

1.6.4 Mice

Natural mutations in Pmel occur in silver mice and a line of mice has been genetically manipulated to be Pmel null [64, 65].

A naturally occurring one base-pair insertion in *Pmel* in the CYT of silver mice is the mutation in *Pmel* that is thought to cause the change in coat colour from a dark fur to a grey fur. However, there are several other Pmel missense mutations in silver mice that were found to be associated with this phenotype (Figure 7d) [65]. When the hairs are closely observed on these silver mice, some of the hairs were found to be completely devoid of pigment, some were sparsely pigmented, while other hairs had a scattered pattern of pigmentation[64].

When a knockout model of Pmel was created, the mice had no major pigment defects[64]. However, when the melansomes in the RPE of these mice were observed it was found that their shape was altered from ovular to spherical, implicating structural defects in Pmel due to Pmel's role in melanosome shape[64].

Other than the melanosome shape being altered in the RPE, no other ocular abnormalities have been documented for either the silver mouse or the null mouse.

The major difference in appearance between these *Pmel* mutant mice lines could be attributed to the location of the mutation, where mutations in the cytoplasmic region can cause major changes in global pigmentation, while mutations earlier in the protein may cause minor changes in global pigmentation. This theory is supported by the plumage change in different chicken PMEL mutants.

1.6.5 Chickens

Many breeds of chickens have numerous mutations in PMEL, but only three plumage types have been directly associated with mutations in PMEL (Figure 7e)[66].

One allele that is causative of these plumage morphs is dominant white. This allele is incompletely dominant to the wild type allele. Homozygotes with this mutation have completely white plumage, but no other documented pigmentation defects. The mutation that causes this phenotype is an insertion of three amino acids, WAP, at amino acid residue 723 in the CYT. In addition to this causative mutation, the dominant white allele also has a missense mutation, N399D, but this mutation has not been linked directly with the plumage change[66].

The second allele is smoky. The smoky allele results from a deletion of four amino acids, Δ280-283 PTVT, in the RPT. The smoky allele is derived from the dominant white allele, meaning that the three amino acid insertion at amino acid residue 723 and N399D missense mutation also occurs in this allele. The plumage of the *smoky* chicken is a gray, slightly mottled colour, reverting the complete lack of

26

pigment that is caused by the dominant white allele. The effect of the four amino acid deletion alone is currently unknown since it does not occur independently of the three amino acid insertion[66].

The last allele affecting plumage colour through mutations in PMEL is dun. The dun allele is derived separately from the dominant white and smoky alleles. The allele has several missense mutations in PMEL: A35V, G105S, and R740C, and one five amino acid deletion. Due to its proximity to the causative mutation in the dominant white allele, it is speculated that the causative mutation in the dun allele is the five amino acid, LGTAA, deletion at amino acid residue 731 in the CYT. The plumage of a heterozygote *dun* chicken is a light brown colour while the plumages of homozygotes are closer to white. However, it is interesting to note that the R740C missense mutation is homologous to the missense mutation found in horses that was found to be causative of the silver dapple phenotype[66].

Although no overt ocular phenotypes in chickens have been found to be in association with PMEL, in a study that investigated melanosomes in phenotypically *dominant white* chickens abnormalities in melanosome formation were found. There was a reduced number of melanosomes present and of the melanosomes present, much like what was found in the Pmel null mice, were more spherical in shape. In addition, the melanosomes did not appear to be as pigmented as would be expected[69].

1.6.6 Zebrafish

Unlike the other animals that were listed, a forward screen for an ocular phenotype in zebrafish rather than a change in global pigmentation identified PMEL

as a causal gene for both phenotypes[67]. The zebrafish line that was discovered to have a non-sense mutation, E390*, in the RPT of one of its two PMEL orthologs, pmela, is called *fading vision* (Figure 7f)[67]. These zebrafish have a global reduction of pigment, which includes the RPE. They were also identified to have trouble swimming[67], and have microophthalmia[71]. In a study looking at *pmela* morphants, it was found that the melanosomes in the RPE of injected individuals were more spherical in shape than what was to be expected, as was observed in mice and chickens[70].

Table 2: Mutations in PMEL Found in Animals

Animal	Mutation	Location	Phenotype
Cattle	Del.18 L	SP	Diluted Coat Colour
	G22R	SP	Diluted Coat Colour
	A610E/A612E	CYT	Unassociated
Horses	R625C	CYT	Silver Dapple, Ocular Anomalies
Dogs	Retrotransposon Insertion	TM	Merle, Ocular Anomalies
Mice	S170L	NTR/CAF	Silver
	R175G	NTR/CAF	Silver
	D373N	RPT	Silver
	F471S	KLD	Silver
	Ins. 603 fs.	CYT	Silver
	Deletion of Exon 2 and 3	NTR	Very Minorly Diluted Coat Colour, Altered Melanosome Structure
Chickens	N399D	PKD/RPT	White, Gray, Altered Melanosome Structure
	Ins. 723 WAP	CYT	White, Gray, Altered Melanosome Structure
	Del. 280-283 PTVT	PKD	Gray
	A35V	NTR	Dun, White
	G105	NTR/CAF	Dun, White
	Del. 731-735 LGTAA	CYT	Dun, White
	R740C	CYT	Dun, White
Zebrafish	E490*	RPT	Global Pigment Reduction, Ocular Anomalies

In summary, the animal models show us that PMEL is heavily involved in the colouration of the main body, but not in all pigmented structures. In some animal models, mutations in PMEL also affect normal ocular development, indicating that PMEL has a role in defining ocular structure. When indicated that the melanosomes in the RPE were observed, mutations in PMEL in animal models alter normal melanosome shape even if overt eye structure does not seem to be altered.

1.7 The Zebrafish Animal Model

Zebrafish were chosen as an animal model to study PG/PDS due to the following factors.

First, the zebrafish has a similar ocular structure and function to that of humans. To be able to study a human disease in zebrafish, the structures that the disease affects in humans must be understood in zebrafish. Zebrafish have been used to study vertebrate embryology and development and they have many developmental similarities to humans [72-74]. In particular, the ocular system of zebrafish functions very similarly to that of the human ocular system which has allowed for the use of zebrafish in the study of many different human ocular diseases[73-77]. In the study of glaucoma, the zebrafish animal model has historically not been as popular as other animal models[78]. Its lack of popularity is attributed to the zebrafish's phylogenetic distance from humans and some differences in anatomy that do not have to be considered in models such as the mouse. However, due to the relative ease of the zebrafish animal model, the focus towards using the zebrafish animal model is shifting[78, 79]. In addition, the zebrafish animal model has come to the forefront as an excellent model to study toxicology and for the *in vivo* screening

of therapeutic drugs, which can be useful in the discovery of treatments for glaucoma[72, 76, 80-83].

The ease of the genetic manipulation of the zebrafish animal model is another reason why we chose the zebrafish animal model to study the role of PMEL in PG/PDS. Zebrafish are genetically tractable, with a sequenced and well characterized genome[73, 74]. Many tools have been developed to work with zebrafish, of which can be accessed for this study. Zebrafish are also highly fecund, fertilize externally, and develop quickly[84].

Zebrafish do, however, possess one significant hurdle. Zebrafish are part of a lineage where there was a genome duplication[85, 86]. One of the genes that were affected by this duplication was PMEL. Therefore, in zebrafish there are two paralogs of PMEL, *pmela* and *pmelb*[67, 70]. Although both pmela and pmelb are longer in sequence than PMEL, like PMEL orthologs in other animals, the protein domains are well conserved[70].

1.8 Studying Glaucoma Using the Zebrafish Eye

To understand the effects of mutating *pmela* or *pmelb* on the health of the zebrafish eye and how those phenotypes correlate to how PMEL may cause PG/PDS in humans, we need to understand the strengths and limitations of working with the zebrafish eye.

The zebrafish eye does not fully develop until 3 days post fertilization[75]. Focusing on the anterior segment, there is a high degree of similarity between the development of the zebrafish eye and the human eye (Figure 8) [86, 87]. This similarity in development also means a high conservation of ocular structures between the zebrafish and human anterior segments[87]. Many genes that are involved in the development of the human eye are also involved in the development of the zebrafish eye[87]. Other strengths of the zebrafish model in the study of PG/PDS, is the conservation of the pigmentation of the iris

and the placement of the zonules in the zebrafish eye[88]. In terms of studying glaucoma and the risk factor of high intraocular pressure, it has been found that zebrafish have a similar intraocular pressure to that of humans[87, 89, 90].

Limitations of the zebrafish model in studying glaucoma are the differences that are associated with aqueous humour outflow. The production of aqueous humor in the posterior chamber of the eye is highly conserved between humans and zebrafish, but there is a dorsal preference for production in zebrafish[75, 91]. In terms of aqueous humor outflow, in humans, the collector channels are circumferential; in zebrafish there is a ventral preference for the collector channels[75, 91]. In addition, zebrafish do not have a structure that is analogous to the trabecular meshwork found in humans. Instead, the closest structure they have is the annular ligament, which completely develops closer to adulthood (Figure 7a,b)[75, 86, 88, 92]. The annular ligament is composed of a different set of proteins than the trabecular meshwork and also has a different ultra structure that does not seem to be involved in drainage but rather in maintaining the structure of the anterior segment[75, 88, 92]. However, the annular ligament does provide a structure by which the aqueous humor has to flow through in order to exit the eye; the general movement and drainage of the aqueous humor in zebrafish is very similar to that in humans other than the dorsal to ventral preference[75, 86, 88, 91]. In addition, although this structure is not part of the eye itself, the canalicular network of the zebrafish eye, located in the canals exiting the eye, has been shown to be functionally homologous to the trabecular meshwork[90]. It is important to take these differences into account when investigating the role of the trabecular meshwork in a disease such as PG/PDS.
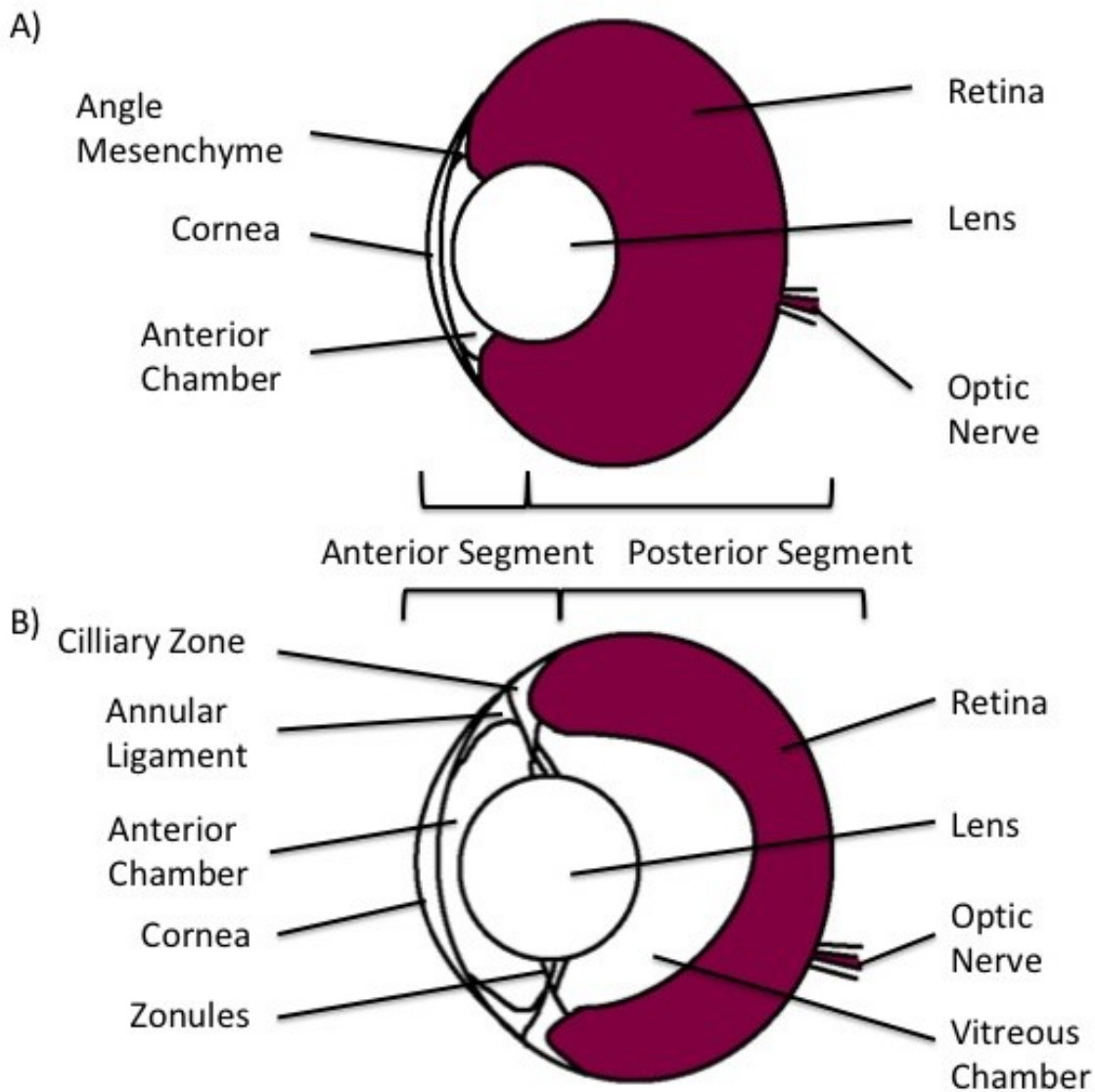
Figure 8: The larval and adult zebrafish eye.
A) *The larval zebrafish eye (pre-17 days post fertilization) does not have all of its structures fully developed and are less than a millimeter in axial length[93]. The anterior segment holds the angle mesenchyme, the cornea, the anterior chamber, and the lens. The posterior segment is composed mostly of retina.* **B)** *The adult zebrafish eye has many more structures and is typically two millimeters in axial length[93]. The anterior segment develops the annular ligament. The cilary body and zonules becomes more pronounced, as does the anterior chamber. The annular ligament is analogous to the trabecular meshwork in functiom. The posterior segment develops a vitreous chamber.*

1.9 Morpholinos

Morpholinos (MOs) are a genetic tool used for the transient knock down of mRNA products. They are composed of modified antisense sequences designed to bind to mRNA. MOs bind to pre-mRNA sequences and inhibit the proper translation process in one of two ways. The first way is by inhibiting translation all together; these are translation-blocking MOs. The MO sequences for these types of MOs typically target the region in the pre-mRNA that comes before the first exon(Figure 9a). By doing this, the MO inhibits the ability for ribosomes and other cell machinery to translate the mRNA sequence[94]. Splice blocking MOs target the pre-mRNA at splice sites with the intention of blocking the proper functioning of a splice site, resulting in the inclusion of an intron or the skipping of an exon (Figure 9b)[84].
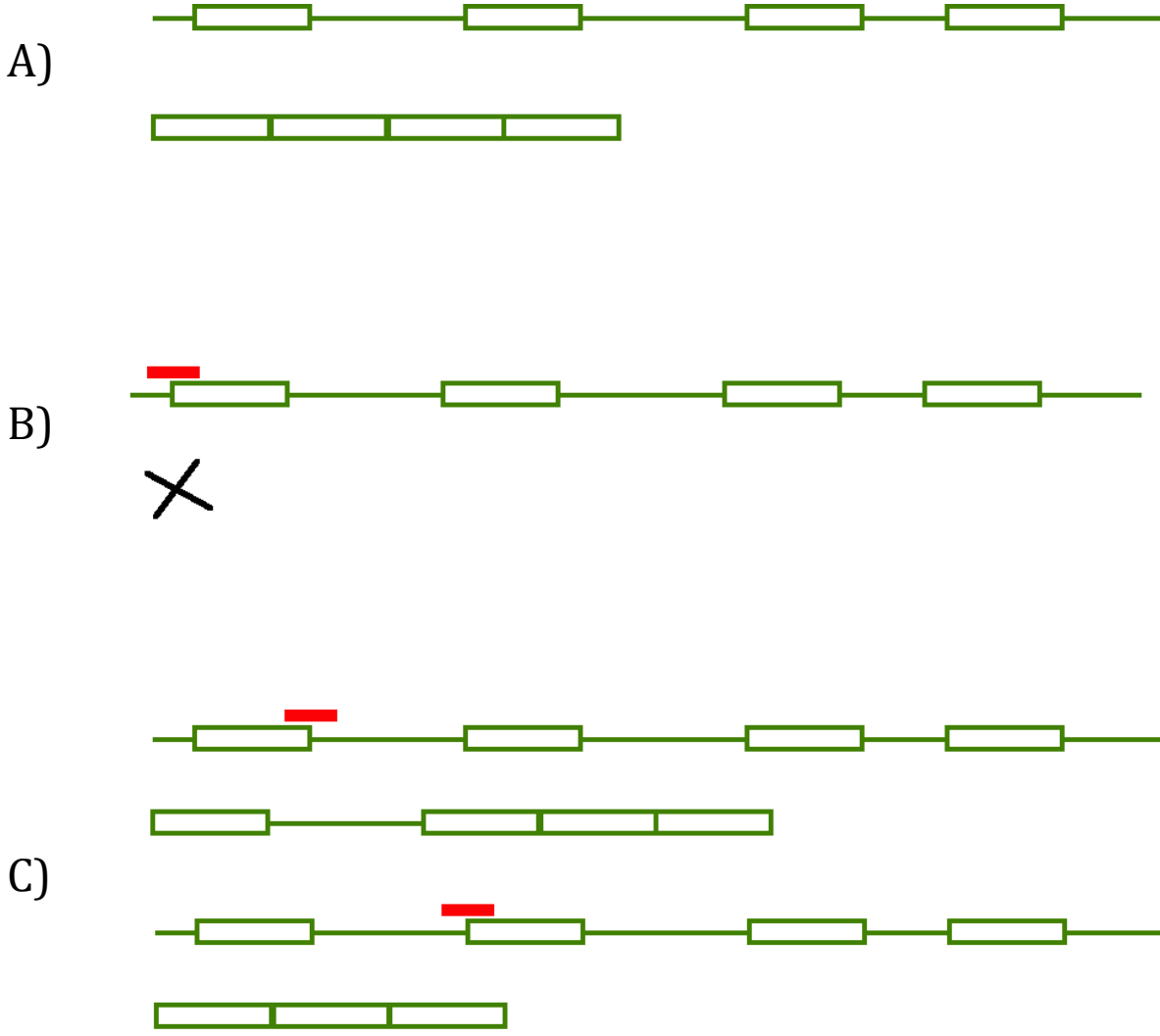
Figure 9: Types of morpholinos and their modes of actions.
A) The normal translation of pre-mRNA to protein without a morpholino present. Introns (lines) are excluded from the protein while exons (boxes) are included in the resulting protein. B) Translation blocking morpholinos target the 5'-untranslated region, blocking translation machinery producing no protein. C) Splice blocking morpholinos target splice sites, either inducing the inclusion of an intron or the exclusion of an exon in mature mRNA, which is then translated producing aberrant proteins.

MOs can be toxic, cause abnormal phenotypes, and produce off target effects which can erroneously be ascribed to the original target. In order to circumvent this problem, it is important that MOs be used with proper controls in place, such as the use of a scramble control MO as a comparator[84, 94, 95]. However, when controlled properly, MO's are a useful tool in determining short-term phenotypic effects in a limited period of time. Also, having a phenotype produced by MOs to compare to phenotypes produced by CRISPR/Cas9 can aid in determining if phenotypes may be caused by off target effects in either method.

In addition to having *fading vision* as precedence to manipulating PMEL in zebrafish, MO experiments have already been performed by two separate labs that have indicated the efficacy of knocking down *pmela*[67, 70]. Not only has a reduction in the pigmentation of the RPE been seen[67], but also the altered shape of melanosomes in the RPE due to *pmela* morpholino injection[70]. Although a *pmelb* MO has been created, there was no evidence that the MO was efficacious; slight differences were found when the *pmelb* MO was combined with the *pmela* MO but there were no significant differences caused by the *pmelb* MO alone [70].

1.10 CRISPR/Cas9

CRISPR/Cas9 is currently the newest, fastest, and easiest form of genetic manipulation on the market. Prior to CRISPR/Cas9, techniques such as zinc-finger nucleases (ZFN) and transcription activator-like effector nucleases (TALENs) were used in order to create stable genetic lines, but those techniques were both more costly and less time effective[96-102].

CRISPR/Cas9 originated from a study on the response of bacteria and archea in the face of invading viruses[100, 102-105]. CRISPR stands for clustered regularly interspaced

short palindromic repeats and Cas9 is an enzyme that has the ability to cut at these CRISPR sites.

In bacteria, this system is used as a defense. When the bacteria encounters an invader, and survives, it then stores portions of the intruders DNA for future identification of the invader, somewhat like how humans create antibodies. Unlike human antibodies, these sequences can be inherited by the next generation of bacteria[103, 104]. These DNA segments are the CRISPR sequences. When the invader appears again, the bacteria uses these stored sequences of DNA to hone in on intruder DNA and then with Cas9, cuts the foreign DNA, rendering the intruder unable to properly replicate[100, 103, 104].

Using this targeted response, we can manipulate the CRISPR/Cas9 system to target any region of DNA as long as the CRISPR and the Cas9 protein is designed and chosen with care[99, 106-108]. There are now several different spin offs of CRISPR technology that aim at using CRISPR in specific ways, but the most basic technique that will be utilized in this study is non-homologous end joining (NHEJ). The CRISPR site that is chosen for NHEJ does not have many limitations, a major one being the presence a proto-spacer adjacent motif (PAM) site beside the CRISPR site. The PAM site is not part of the CRISPR sequence, but it is a requirement for the CRISPR/Cas9 complex to adhere to the DNA, and therefore, make the cut[102, 109-111]. In NHEJ, the cut sequence is then left to use the cell machinery to repair itself. As can be expected, an uncontrolled repair of the DNA could result in many different effects ranging from creating synonymous mutations to cell death. If a person using CRISPR/Cas9 is hoping for a large effect, an out of frame insertion or deletion is usually the sought after result[99, 102, 106, 112].

Although the organism is usually targeted at a single cell stage, so that if a mutation were to be introduced it will be replicated in every cell of the organism, often times the cell will replicate before the CRISPR/Cas9 can create one stable DNA template. This means that the CRISPR/Cas9 system can and will act differently in different cells creating many mutations. In NHEJ, you will get cells with a variety of different mutations within one organism. The F0 generation of modified organisms is therefore considered mosaic. If they do not have any mutations in their germ line, they are not further useful. However, if they do have mutations in their germ line, the mosaic organisms can be used to create stable mutant lines through breeding (Figure 10).
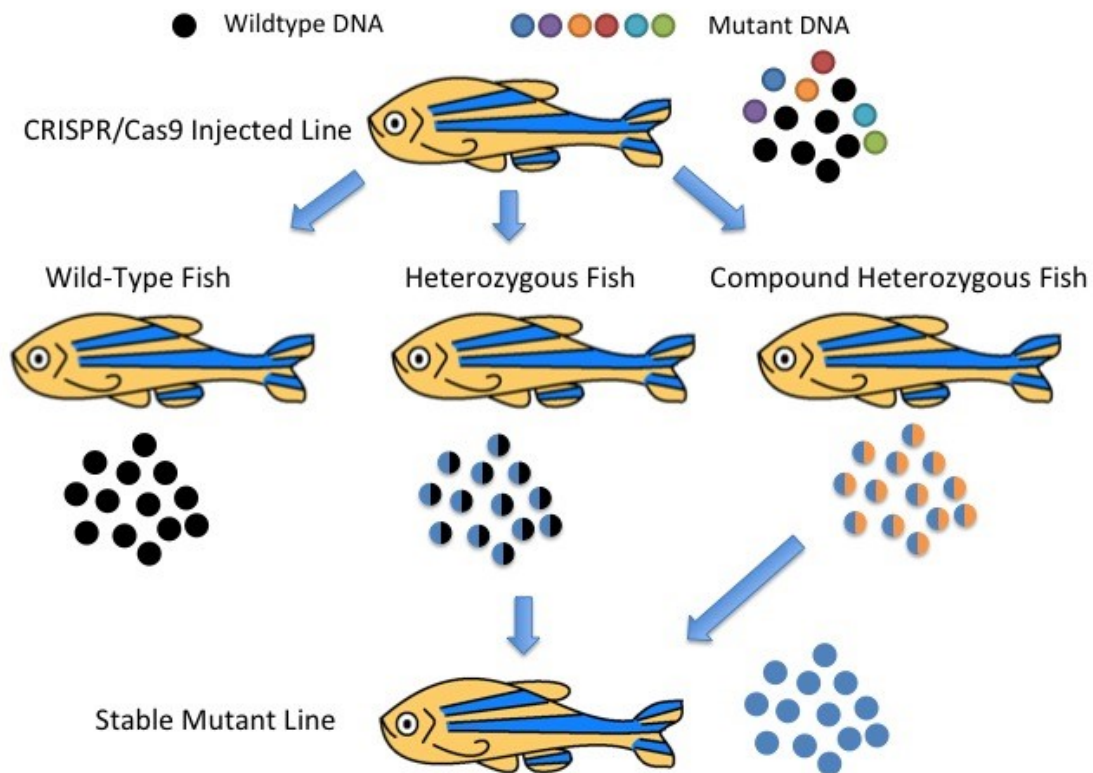
Figure 10: CRISPR/Cas9 can produce mosiac organism, which can be bred to stable mutant lines.

A CRISPR/Cas9 injected organism, even if injected at the one cell stage, may develop to have populations of cells with different mutations if the cells divide before the CRISPR/Cas9 system is able to stably alter the DNA. In order to develop a stable line, these "mosaic" CRISPR/Cas9 injected organisms (F0) can be bred to each other or to a wild type line. The result of breeding mosaic organisms can be homozygous wild type organisms, heterozygous mutant organisms, compound heterozygous mutant organisms, or homozygous mutant organisms (F1). If no homozygous mutant organisms are bred from two mosaic organisms, then heterozygous mutant organisms or compound heterozygous organisms with the same mutation can be bred with one another to produce ~25% homozygous mutants.

Currently, the biggest problem with CRISPR/Cas9 is the possibility of unknown off target affects[102, 113, 114]. Programs that are used to design CRISPR sequences can predict the specificity of the target, but it has been shown that *in silico* predictions are not reliable, although work is being done to improve them[115, 116]. Off-target cutting means that although a particular gene, or section of a gene, is being targeted, that the CRISPR/Cas9 system can target and cut in other areas of the genome causing effects that are unrelated to the gene that is being studied. Many efforts are currently being made to modify the CRISPR/Cas9 system so that off target cutting and off target effects can both be detected and then minimized[106, 117-119].

CRISPR/Cas9 has been adapted for use in many different models including zebrafish[101, 109, 120-122]. There are several different technologies that are available to find appropriate CRISPR sites in zebrafish. The short generation times, and short duration of development for zebrafish, compared to mammals, allow for the easier breeding out of off target cutting and for the development of stable lines.

Creating a stable zebrafish mutant via CRISPR/Cas9 has many benefits. Although using CRISPR/Cas9 to create a stable mutant initially takes more time than injecting MOs at the beginning, once a stable line of zebrafish is established, mutant zebrafish simply need to be bred rather than created during each experimental round. A stable mutant will allow us to be able to investigate any phenotypes that result from the mutation at different life stages, whereas MOs only allow us to observe phenotypes in zebrafish hatchlings. MOs are also limited by their toxicity and potential off target affects that can be bred out of a stable mutant line of zebrafish. We can also avoid pitfalls in MO injection such as the effects of minute dosage differences in phenotype. Creating a stable mutant line allows more

flexibility in terms of experimentation; we don't have to worry about the interaction of different injected chemicals meant for diagnosis, rescue, or treatment in stable mutants.

1.11 Hypothesis and Aims

Mutations in PMEL are strongly associated with PG/PDS. To test the hypothesis that patient mutations in PMEL are causative of PG/PDS, we sought to disrupt PMEL in an *in vivo* model. We predicted that creating mutations in PMEL homologs in zebrafish would result in phenotypes that would resemble the phenotypes seen in patients with PG/PDS. By observing how mutant PMEL causes eye abnormalities in zebrafish, we can begin to understand how PMEL is involved in the process of PG/PDS. Understanding the mechanism of disease development and how these mutations can cause PG/PDS in the visual system would be the first step to identifying other genetic causes of PG; it would also expand our knowledge of glaucoma etiology, and lead to novel diagnostic and treatment options for this major cause of debilitating blindness worldwide.

To begin addressing this hypothesis, the following two aims were designed and accomplished:

1) The transient knock-down of *pmela* and *pmelb* through the use of MOs. In two previous studies[67, 70], *pmela* had been knocked down using MOs. In one of those studies, *pmelb* was also knocked down using MOs[70]. However, these two studies did not observe for the same effects. In this aim, we sought to characterize how the two *pmela* MOs affected global pigmentation and if we would be able to make a more efficacious *pmelb* MO.

2) The stable knock out of pmela using CRISPR/Cas9. MOs create transient knock downs. However, in order to study a disease that usually appears in old age, a stable knock out of *pmela* needed to be created and then characterized. To create this stable knock out,

we used the CRISPR/Cas9 system to target what seems to be the dominant PMEL paralog, *pmela*, and screened for phenotypes that could be associated with PG/PDS. The hatchling stages of these knock out zebrafish can be compared to morphants to support that off target effects of the MOs or the CRISPR/Cas9 are not the reason for the phenotypic changes.

Chapter 2: Materials and Methods

Portions of this chapter were written for "Non-Synonymous variants in Premelanosome Protein (PMEL) cause ocular pigment dispersion and pigmentary glaucoma." Adrian A. Lahola-Chomiak *et al.* (Submitted)

2.1 Zebrafish Husbandry

All zebrafish husbandry and experimentation were completed under Protocol #AUP00000077 approved by the University of Alberta Animal Care and Use Committee: Biosciences under the auspices of the Canadian Council on Animal Care. Zebrafish were maintained at 28.5°C in standard conditions[123-125].

2.2 Morpholino

Antisense morpholino oligonucleotides (MO) were purchased from Gene Tools, LLC. Two *pmela* MOs, one *pmelb* MO, and one control MO were used for this experiment (Table 3). The MOs were mixed for injection as follows: 2.5 μL of MO, 2.5 μL of phenol red, 1.0 μL of 0.1 M KCl, and 4.0 μL of MilliQ water. The injection solution was delivered to 1 or 2 cell stage zebrafish embryos by injection into the yolk[126]. Each embryo received 10 ng of MO total; however, one test group exception was made in the co-injection of *pmela* MO2 and *pmelb* MO2 at high dosage, where a total of 20 ng of MO, 10 ng of *pmela* MO2 and *pmelb* MO2, was delivered to the test group.

Table 3: Antisense Morpholino Oligonucleotide Sequences

Gene	Version	Morpholino Sequence	Reference
pmela	MO1	5'-GAGGAAGATGAGAGATGTCCACATG-3'	Schonthaler *et al.* (2005)
pmela	MO2	5'-GATGAGAGATGTCCACATGATGACC-3'	Burgoyne *et al.* (2015)
pmelb	MO2	5'-AGGAAACAGTGTTTACTTACTTGTT-3'	----
control	SC	5'-CCTCTTACCTCAGTTACAATTTATA-3'	Gene Tools, LLC

2.3 Reverse Transcription

The reverse transcription of *pmelb* mRNA transcripts to cDNA was performed using the Superscript IV VILO Mastermix (Thermofisher, 11756050). The *pmelb* cDNA was then sequenced with the following primers: 5'-AGTGCCAACAAAGTGACACA-3' and 5'-AACCGCAAAGGGAATCTGGT-3' ordered from Integrated DNA Technologies, Inc (IDT).

2.4 CRISPR/Cas9

To produce guide RNA, the CRISPR binding sequence (Table 4) for the cytoplasmic domain of *pmela* was designed in Geneious 9.1.8 (Biomatters Limited). An SP6 promoter and gRNA backbone (Table 4) was added to this sequence and then the resulting oligomer was annealed to the constant oligomer (Table 4). The annealing procedure was performed by mixing $\sim$100 µM of the gene-specific sequence and $\sim$100 µM of the constant oligomer and heating it to 95℃ for five minutes before reducing the temperature to 85℃ at 2℃/second and then to 25℃ at a rate of 0.1℃/second. The oligonucleotides were ordered from IDT. The resulting oligonucleotide was then transcribed into guide DNA with T4 DNA polymerase (New England Biolabs, M0203S) by adding 2.5 µL of 10mM dTNPs, 2 µL of 10x NEB Buffer 2, 0.2 µL 100x NEB bovine serum albumin, 0.5 T4 NEB DNA polymerase, and 4.8 µL of MilliQ water and then incubating the solution at 12℃ for 20 minutes. The DNA was purified (QIAquick PCR Purification Kit, Qiagen, 28104), and further transcribed and purified using the mMessage Machine SP6 transcription kit (ThermoFisher Scientific, AM1340)[109]. Zebrafish embryos at the 1 cell stage were injected with 1 nL of a cocktail containing 1 µL of guide RNA (at >2000ng/µL) mixed with 2 µL of Cas9 protein stock (New England Biolabs, M0386S), 0.5 µL Cas9 buffer (New England Biolabs, M0386S), and 1.5 µL 1.5M KCl. After cutting of the target genomic region was confirmed in injected embryos

using the polymerase chain reaction (PCR) primers listed in Table 3, other injected

embryos were raised and their progeny were assessed for mutations surrounding the

target region.

Table 4: CRISPR/Cas9 Oligonucleotide and Primer Sequences

Sequence Description	Oligonucleotide Sequence
CRISPR Binding Sequence	5'-GATAACGTGCAAATCGAGTT-3'
SP6 Promoter	5'-ATTTAGGTGACACTATA-3'
gRNA Backbone	5'-GTTTTAGAGCTAGAAATAGCAAG-3'
Constant Oligomer	5'-AAAAGCACCGACTCGGTGCCACTTTTTCAAGTTGATAACGGACTAGC CTTATTTTAACTTGCTATTTCTAGCTCTAAAAC-3'
pmela PCR Forward Primer	5'-CAGGCGGTTTAAGGAGTACCA-3'
pmela PCR Reverse Primer	5'-GTGACTGTAGACCAAATAAAGCAG-3'
pmela qPCR Forward Primer	5'-GCGACACTCGGAGTTCTGTT-3'
pmela qPCR Reverse Primer	5'-TCACACCACGCGTCCCAGCA-3'
pmelb qPCR Forward Primer	5'-CAATGACTCTGGAACCTTCTG-3'
pmelb qPCR Forward Primer	5'-ACGACAGTCAAGATCCCCAAC-3'

2.5 DNA Isolation and Sequencing

Mosaic zebrafish larvae were pooled into groups for DNA extraction and sequencing. DNA was extracted from individual fish for genotype sequencing.

Zebrafish DNA was isolated by adding 50mM NaOH and then boiling the zebrafish tissue at 95℃ for 10 minutes. Samples were then chilled on ice before 1/10th of a volume of 1M Tris-HCl was added to the solution. The supernatant containing the DNA was then isolated by centrifugation at max speed[127].

For DNA samples where individual strands needed to be sequenced, the isolated DNA underwent an initial round of PCR (Table 4) (Taq DNA Polymerase Kit, Qiagen, 201203) and then cloning (TOPO TA Cloning, Invitrogen/Thermofisher, K4500-01SC). The cloning process would ensure the sequencing of single strands of DNA. A transformation (OneShot TOP10, Invitrogen) was then performed by mixing 16.7 μL of cells with 6 μL of plasmid, leaving the solution on ice for 30 minutes, and then heat shocking the cells for 30 seconds at 42℃. The cells were then placed on ice for an additional two minutes before 250μL of Super Optimal Broth was added and the resulting solution was incubated at 37℃ on a shaker for 1 hour. Cells were then plated on luria broth agar (Fluka, 52062) plates with canamycin antibiotic. Plasmids were isolated (QIAprep Spin Miniprep Kit, Qiagen, 27106) and sequenced using Standard Sanger DNA sequencing (Table 4).

2.6 Binarization

Morphology of zebrafish was assessed and documented with a Leica MZ16F stereo-dissection microscope with a mounted 12.8 megapixel digital camera (DP72, Olympus). Images were converted to 32-bit gray scale using ImageJ (Wayne Rasband, National

Institutes of Health). Quantification of pigmentation was performed by binarization of images in ImageJ[123].

2.7 Quantification of Pigmentation and Ocular Structure

All images were taken from a dorsal point of view and quantified in Image J. Pigmentation was quantified by calculating the percentage of black pixels composing the zebrafish[123]. Body length was calculated by measuring the longest distance from the front edge of the zebrafish larvae head to the tip of the zebrafish larvae tail. The eye length was calculated by taking the longest nasal to temporal distance. The anterior segment of the eye was calculated by measuring the distance between the cornea and the lens. The circumference of the eye was calculated by measuring the outer edges of the eye.

2.8 qPCR

RT-qPCR on zebrafish larvae followed the MIQE guidelines for primer validation and RNA quality control[128]. RNA was extracted from 3 days post-fertilization wild type and mutant embryos with the RNeasy Minikit (Qiagen, 74106) and DNase I (Qiagen, EN0521). Wild type embryos were bred from wild type parents and mutant embryos were identified via their phenotype. RNA was assessed for quality on an RNA 6000 NanoChip and 2100 Bioanalyzer (Agilent Technologies). The RNA was then synthesized into cDNA with qScript Supermix (Quantabio, 95048-100). The SYBR green system was used for qPCR on a 7500 Real-Time PCR system (Applied Biosystems) using primers (Table 4) validated to produce a single clean peak and maintain a linear amplification over a broad dilution range. qPCR was performed in three technical replicates on each biological replicate. Transcript

abundance was reported as relative to β-actin levels[124]. Ct values were called and converted to RQ (relative quantification) values using β-actin levels for analysis.

2.9 Genotyping Using Restriction Fragment Length Polymorphisms

Genotyping of the ua5022 allele was accomplished through the use of a restriction fragment length polymorphism (RFLPs)[124, 129]. DNA from an individual underwent PCR (Table 4) and then a restriction enzyme digest using the FastDigest system and the restriction enzyme HpaII (Thermofisher, FD1703). The digest solution was composed of 30 μL of MilliQ water, 5 μL of FastDigest Green Buffer, 10 μL of DNA, and 5 μL of HpaII. Solution was incubated at 37°C for 10 minutes (time may need to be further optimized), and then at 85°C for 5 minutes. Two fragments was expected for the wild type allele, 103 bp and 253 bp, while one fragment was expected for the ua5022 mutant *pmela* allele. No RFLP has yet been developed for the ua5021 allele.

2.10 Statistical Analysis

One-way ANOVAs ($p < 0.05$) were performed in Prism 7 (GraphPad) and were used for MO data sets where several different test groups were being observed at once. Student's T-tests (two tailed, $p < 0.05$) were calculated in Microsoft Excel (for Mac 2011, 14.7.1). Student's T-tests were used in morpholino data sets where there were only two variables being observed (ie. MO1 and SC) and in the comparison of zebrafish pigmentation.

Chapter 3: Results

Portions of this chapter were written for "Non-Synonymous variants in Premelanosome Protein (PMEL) cause ocular pigment dispersion and pigmentary glaucoma." Adrian A. Lahola-Chomiak *et al.* (Submitted)

3.1 Knock-down of *pmela* Causes a Reduction of Pigment in Zebrafish Hatchlings

In this study we used both *pmela* MOs (Figure 11) that had been previously

described in the literature[67, 70]. We observed that *pmela*-MO1 resulted in a significant

($p<0.001$) reduction of global pigment compared to zebrafish injected with standard

control MO at 3 dpf (Figure 12). It was found that the injection of *pmela*-MO2 had a

significant reduction in global pigment compared to uninjected zebrafish at 2 dpf ($p=0.002$)

(Figure 13a) and 3 dpf ($p<0.001$) (Figure 13b). However, the injection of *pmela*-MO2 only

had a significant ($p<0.001$) reduction of global pigment at 3 dpf when compared to the

standard control MO (Figure 13b). In addition to a reduction in global pigmentation, when

the effect of *pmela*-MO2 on the pigmentation of just the eyes was measured at 2 dpf

($p<0.001$, $p<0.001$) (Figure 14a) and 3 dpf ($p<0.001$, $p<0.001$) (Figure 14b), it was found

that the effect on just the eyes was significant compared to uninjected zebrafish and

standard control MO injected zebrafish, respectively.

Although a *pmelb*-MO already exists (*pmelb*-MO1), the literature does not provide

any evidence of the efficacy of that MO. In addition, the efficacy of *pmelb*-MO1 cannot be

easily tested because it is a translation blocking MO rather than splice blocking MO. In

order to test for the efficacy of a translation blocking MO, we would need to be able to

probe for the pmelb protein, for which there is currently no known antibody. Splice

blocking MOs are easier to test for efficacy because the mRNA only needs to be reverse

transcribed and assessed for change in sequence size. In order to attempt to test the

efficacy of a *pmelb* MO, we designed a splice blocking *pmelb* MO (*pmelb*-MO2). This MO was

tested by reverse transcribing mRNA from both control and *pmelb*-MO2 injected zebrafish.

Transcript sizes were examined to check for altered splicing of the mRNA (Figure 15a).

There was no difference in size of transcripts between control injected and *pmelb*-MO2 injected fish (Figure 15b). We found that *pmelb*-MO2 did not result in a significant decrease in global pigmentation or eye pigmentation at 2 dpf or 3 dpf (Figure 13 and Figure 14).

When *pmela*-MO2 and *pmelb*-MO2 were co-injected into AB/Wik zebrafish at a low dosage (a combined 10 ng of MO), there was a significant decrease of pigmentation globally at 2 dpf (p<0.001, p=0.002) and 3 dpf (p=0.001, p=0.03) compared to uninjected and standard control MO injected siblings, respectively. When *pmela*-MO2 and *pmelb*-MO2 were co-injected into AB/Wik zebrafish at a high dosage (a combined 20 ng of MO), there was a significant decrease of pigmentation globally at 2 dpf (p<0.001, p=0.018) and 3 dpf (p<0.001, p=0.001) compared to uninjected and standard control MO injected siblings, respectively (Figure 13).

When *pmela*-MO2 and *pmelb*-MO2 were co-injected into AB/Wik zebrafish at a low dosage (a combined 10 ng of MO), there was a significant decrease in eye pigmentation at 2 dpf (p<0.001, p<0.001) and 3 dpf (p<0.001, p<0.001) compared to uninjected and standard control MO injected siblings, respectively. When *pmela*-MO2 and *pmelb*-MO2 were co-injected into AB/Wik zebrafish at a high dosage (a combined 20 ng of MO), there was a significant decrease in eye pigmentation at 2 dpf (p<0.001, p<0.001) and 3 dpf (p<0.001, p<0.001) compared to uninjected and standard control MO injected siblings, respectively (Figure 14). Interestingly, at 2 dpf, the eyes of low dose and high dose co-injected zebrafish also had significantly less pigmentation than in zebrafish that only had *pmela*-MO2 injected (p=0.028, p=0.043) (Figure 14a).

At 3 dpf in the *pmela* and/or *pmelb* morphants, there were no apparent overtly observed ocular structural defects. Beyond 3 dpf, the observed effect of the MOs was

reduced due to MO degradation in the larval zebrafish. No meaningful observations could

be made about the phenotype of the morphants past 3 dpf.
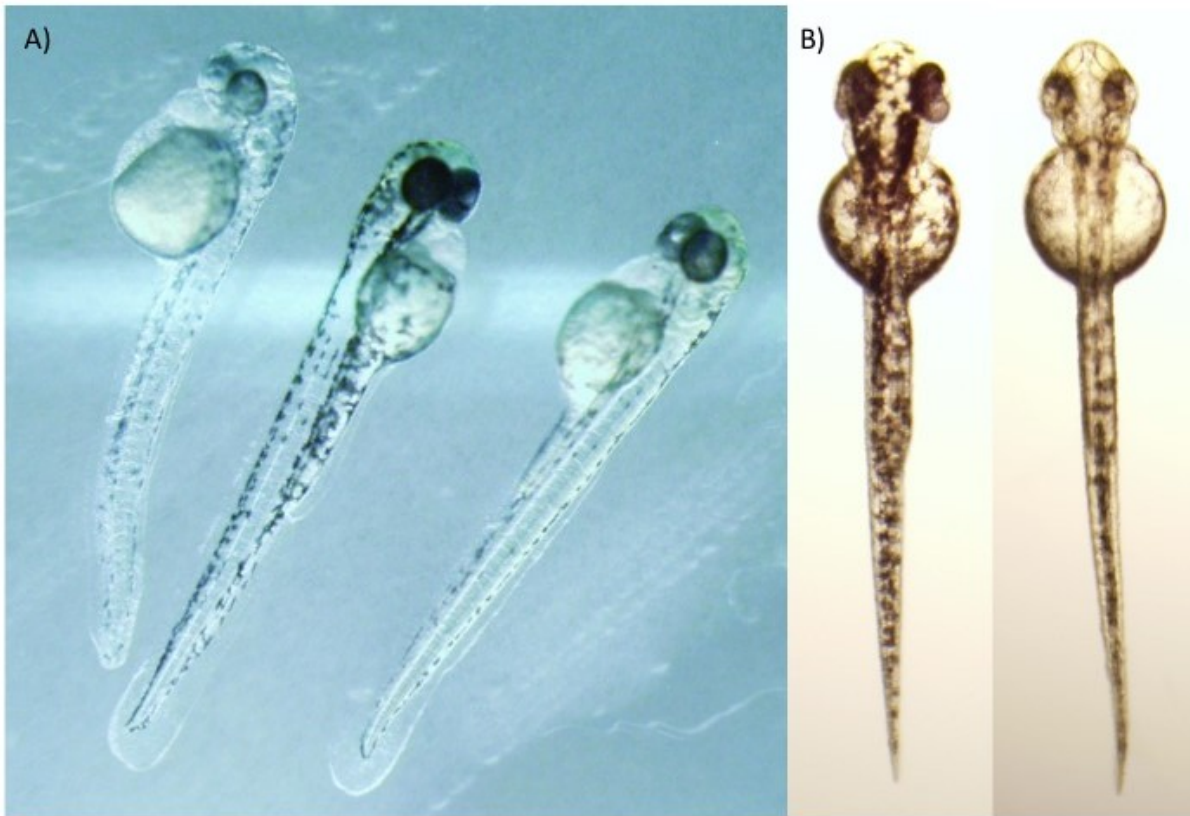
Figure 11: Global reduction of pigment in pmela morphants.
A) Left: 2 days post fertilization (dpf) pmela-morpholino (MO) 1 injected zebrafish. Middle: 2 dpf standard control MO injected zebrafish. Right: 2 dpf pmela-MO2 injected zebrafish. **B)** Dorsal view of pmela morphants. Left: 3 dpf standard control MO injected zebrafish. Right: 3 dpf pmela-MO2 injected zebrafish.

Figure 12: Global reduction in pigmentation in pmela-MO1 injected zebrafish.
Zebrafish injected at the one cell stage with pmela-MO1 have significantly (p<0.001) reduced global pigmentation at 3 days post fertilization when measured by binarization.

Figure 13: Global reduction in pigmentation in pmela-MO2 injected zebrafish.
A) *Zebrafish injected with pmela-morpholino (MO) 2 have significantly less global pigment than uninjected (p=0.002) siblings at 2 days post fertilization (dpf). Zebrafish co-injected with pmela-MO2 and pmelb-MO2 at a low dosage (10 ng total MO) have significantly reduced global pigmentation compared to uninjected (p<0.001) and standard control MO injected (p=0.002) zebrafish. Zebrafish co-injected with pmela-MO2 and pmelb-MO2 at a high do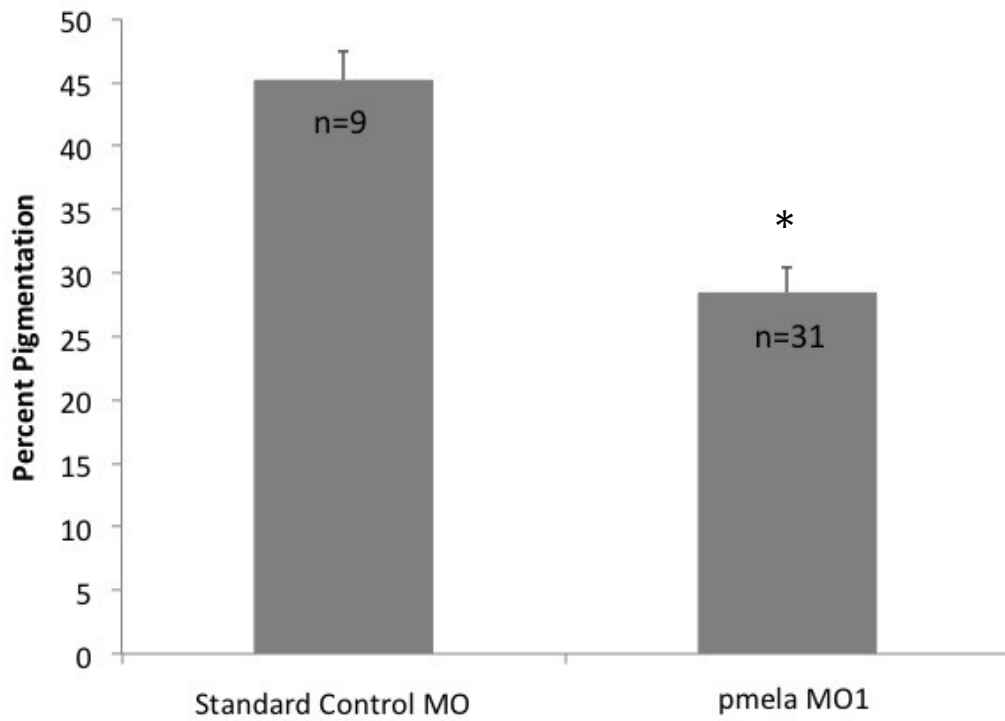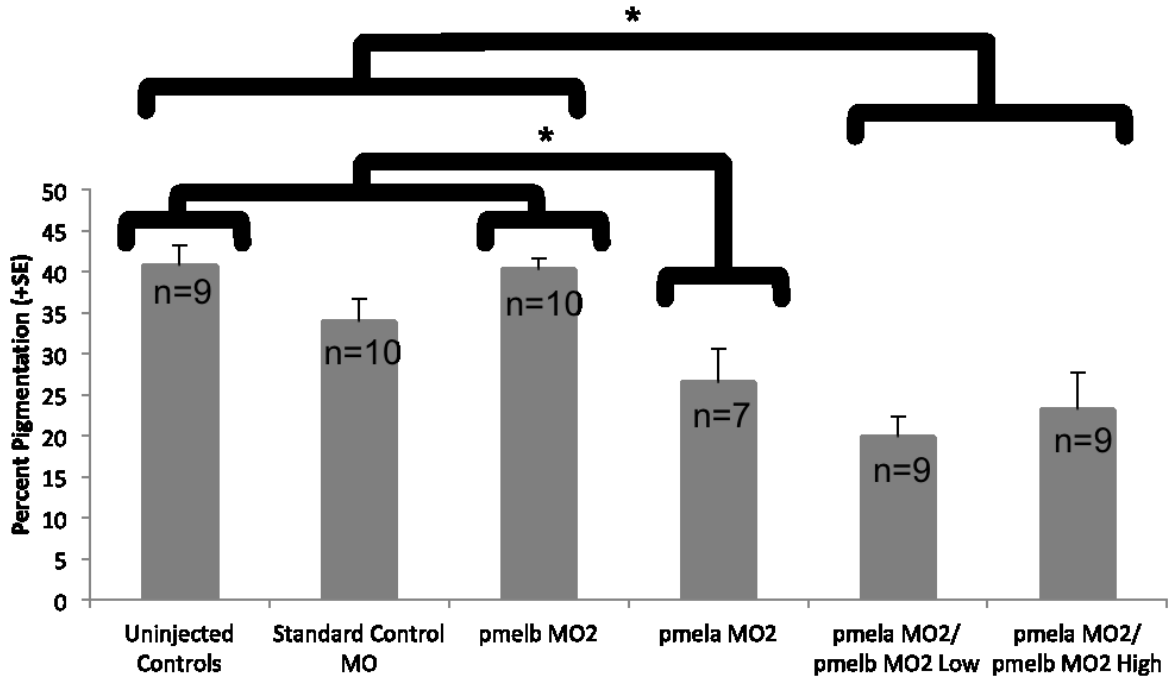sage (20 ng total MO) have significantly reduced global pigmentation compared to uninjected (p<0.001) and standard control MO injected (p=0.018) zebrafish. pmelb-MO2 injected zebrafish do not have significantly reduced global pigmentation compared to uninjected and standard control MO zebrafish at 2 dpf.* ***B)*** *Zebrafish injected with pmela-MO2 have significantly less global pigment than uninjected (p<0.001) and standard control MO injected (p<0.001) siblings at 3 dpf. Zebrafish co-injected with pmela-MO2 and pmelb-MO2 at a low dosage have significantly reduced global pigmentation compared to uninjected (p=0.001) and standard control MO injected (p=0.03) zebrafish. Zebrafish co-injected with pmela-MO2 and pmelb-MO2 at a high dosage have significantly reduced global pigmentation compared to uninjected (p<0.001) and standard control MO injected (p=0.001) zebrafish. pmelb-MO2 injected zebrafish do not have significantly reduced global pigmentation compared to uninjected and standard control MO zebrafish at 3 dpf.*
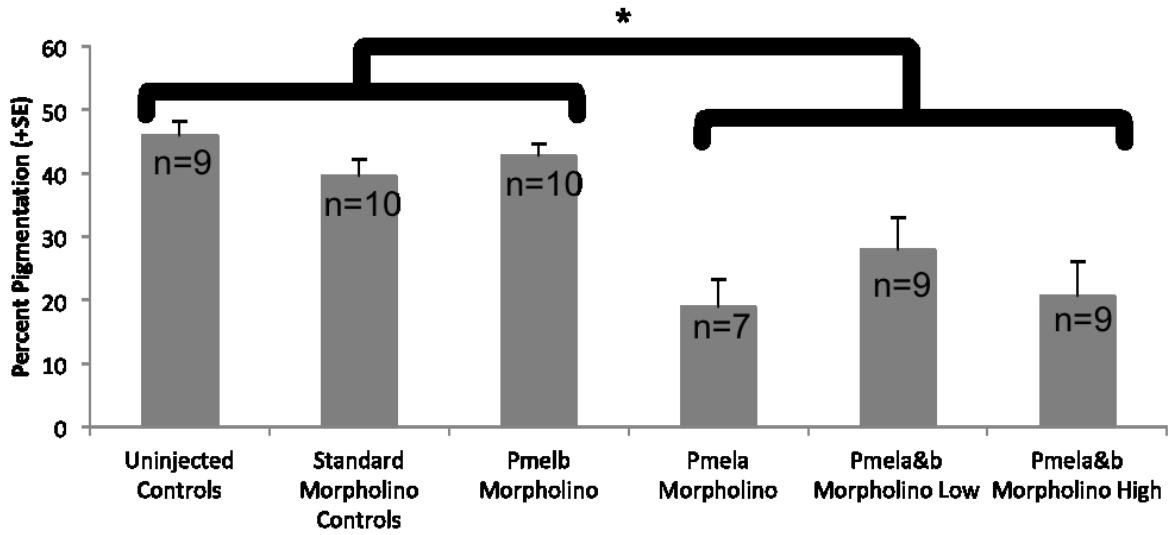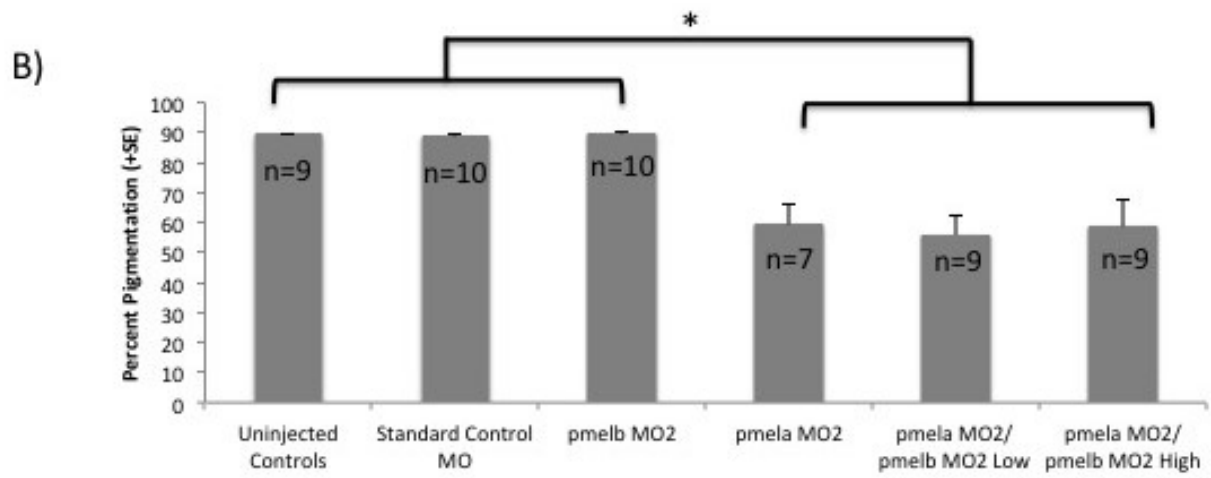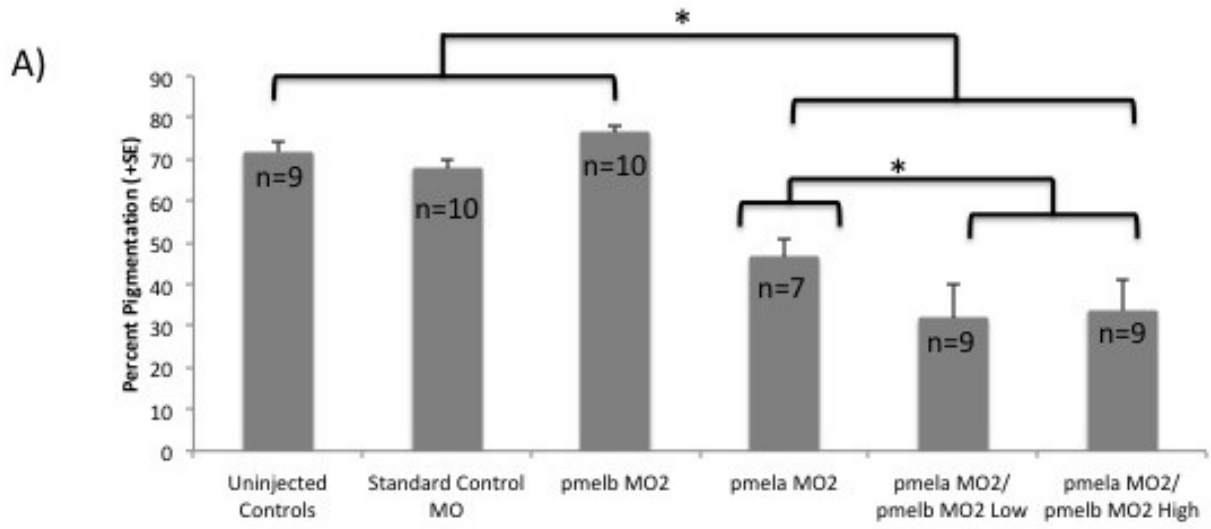
Figure 14: Reduction in pigmentation of the eye in pmela-MO2 injected zebrafish.
A) *Zebrafish injected with pmela-morpholino (MO) 2 have significantly less eye pigment than uninjected (p<0.001) and standard control MO injected (p<0.001) siblings at 2 days post fertilization (dpf). Zebrafish co-injected with pmela-MO2 and pmelb-MO2 at a low dosage (10 ng total MO) have significantly reduced global pigmentation compared to uninjected (p<0.001) and standard control MO injected (p<0.001) zebrafish. Zebrafish co-injected with pmela-MO2 and pmelb-MO2 at a high dosage (20 ng total MO) have significantly reduced global pigmentation compared to uninjected (p<0.001) and standard control MO injected (p<0.001) zebrafish. Zebrafish co-injected with pmela-MO2 and pmelb-MO2 at a low dosage (p=0.028) and at a high dosage (p=0.043) have significantly reduced pigmentation compared to pmela injection alone. pmelb-MO2 injected zebrafish do not have significantly reduced eye pigmentation compared to uninjected and standard control MO zebrafish at 2 dpf.* ***B)*** *Zebrafish injected with pmela-MO2 have significantly less eye pigment than uninjected (p<0.001) and standard control MO injected (p<0.001) siblings at 3 dpf. Zebrafish co-injected with pmela-MO2 and pmelb-MO2 at a low dosage have significantly reduced eye pigmentation compared to uninjected (p<0.001) and standard control MO injected (p<0.001) zebrafish. Zebrafish co-injected with pmela-MO2 and pmelb-MO2 at a high dosage have significantly reduced eye pigmentation compared to uninjected (p<0.001) and standard control MO injected (p<0.001) zebrafish. pmelb-MO2 injected zebrafish do not have significantly reduced eye pigmentation compared to uninjected and standard control MO zebrafish at 3 dpf.*

Figure 15: The pmelb-MO2 is not determined to be efficacious.
A) The properly spliced length of pmelb between the chosen pmelb primers and the splice blocked length of pmelb between the same chosen pmelb primers. B) cDNA transcribed from zebrafish injected with standard control MO (second lane) and pmelb-MO2 (third lane).

3.2 Stable Mutations in *pmela* Created by CRISPR/Cas9

The transient nature of MOs and issues concerning non-specific targeting and MO toxicity makes it difficult to understand the effect of the loss of a gene in later stages of development. In order to better understand the long-term effects of PMEL loss in zebrafish, we engineered stable mutants.

Mutations were engineered in zebrafish using CRISPR/Cas9. We designed multiple guide RNAs to target different regions in *pmela* (Figure 16a, Table 5). DNA from the CRISPR/Cas9 injected zebrafish was isolated, separated into single strands, and sequenced to confirm the presence of mutations. Only one guide RNA was found to be efficacious. This guide RNA was engineered to target the C-terminal region of the zebrafish homologue *pmela* in the CYT (Figure 16a,b). In the pools of injected zebrafish that were sequenced, multiple insertions and deletions in *pmela* were identified. Individual zebrafish were then sequenced and multiple insertions and deletions were once again identified, confirming that the cells of the zebrafish were mosaic in nature (Figure 16b). The genetically mosaic F0 zebrafish did not have any apparent phenotypes as larvae or as adults.

When the adult F0 mosaic zebrafish were randomly bred with each other, approximately 2% of the offspring had a globally reduced pigment phenotype (Figure 16c,d). None of these abnormally pigmented fish survived into adulthood. Phenotypically wild type siblings of these abnormal fish were grown to adulthood and sequenced for the presence of stable heterozygotes.

Table 5: CRISPR Sequences Used to Target pmela

Guide Oligonucleotide #	Sequence	Region
1	5'-GATAACGTGCAAATCGAGTT-3'	NTR
2	5'-GATTTGCACGTTATCGTTCA-3'	NTR
3	5'-GACACAAACAGCGTGCCTCT-3'	NTR/CAF
4	5'-GAATGAACTTGTCTTTGCCG-3'	NTR/CAF
5	5'-GAGCTGCTGAGATAACTGCT-3'	NTR/CAF
6	5'-GACCGAGTTGGAAGCCGAAT-3'	KLD
7	5'-GGCTCTCGGCAGTCGATCTC-3'	CYT
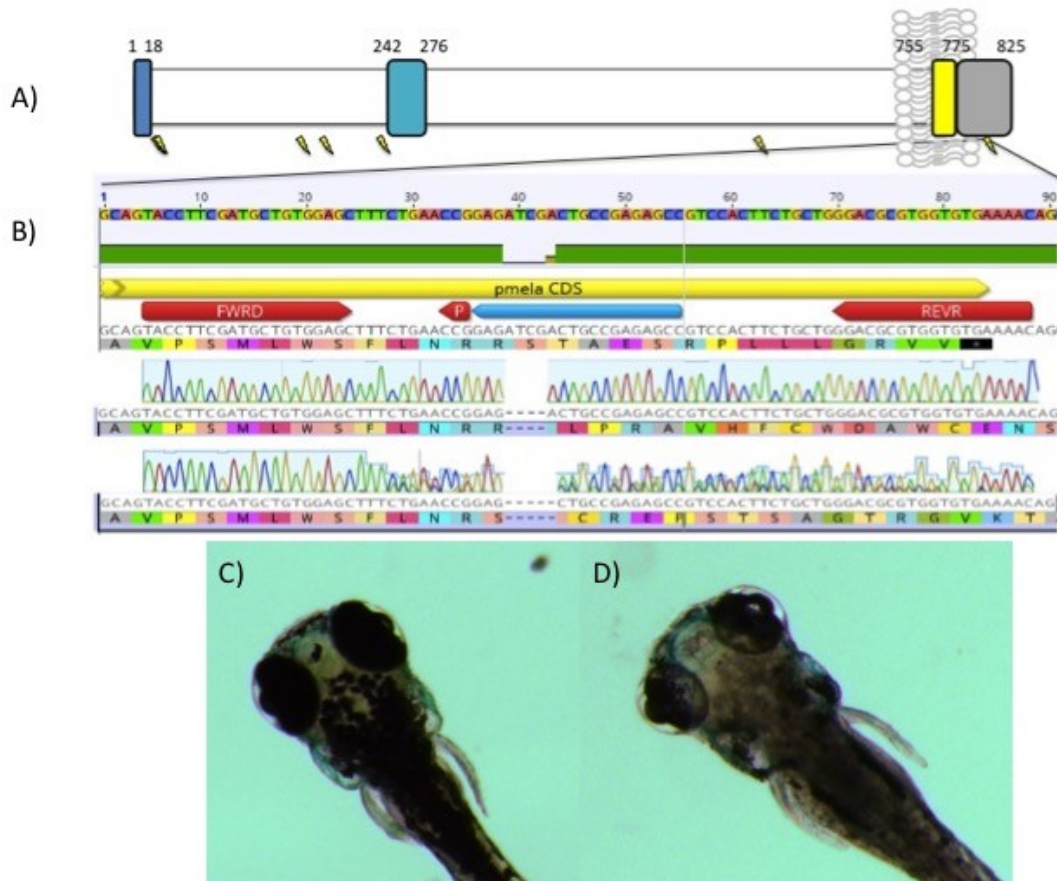
Figure 16: Evidence of CRISPR/Cas9 cutting in the cytoplasmic domain of* pmela *and the offspring of breeding mosaic zebrafish.
A) The seven chosen CRISPR sites in pmela *and the location of CRISPR site 7, where evidence of cutting was found. B) Evidence of cutting. The sequencing information showing two deletions from the same individual indicates the creation of a mosaic zebrafish (F0). C) A phenotypically wild type individual bred from a mosaic cross (F0 x F0). D) A phenotypically mutant individual bred from a mosaic cross (F0 x F0).*

Two stable lines carrying *pmela* mutations were identified in the cohort of siblings: a line with an 11 base pair deletion (allele designation ua5022) (Figure 17a) and a line with a 1 base pair deletion (allele designation ua5021) (Figure 17b). The ua5022 allele results in the loss of three amino acids and a frame shift of two nucleic acids, while the ua5021 allele results in a frame shift of one nucleic acid.
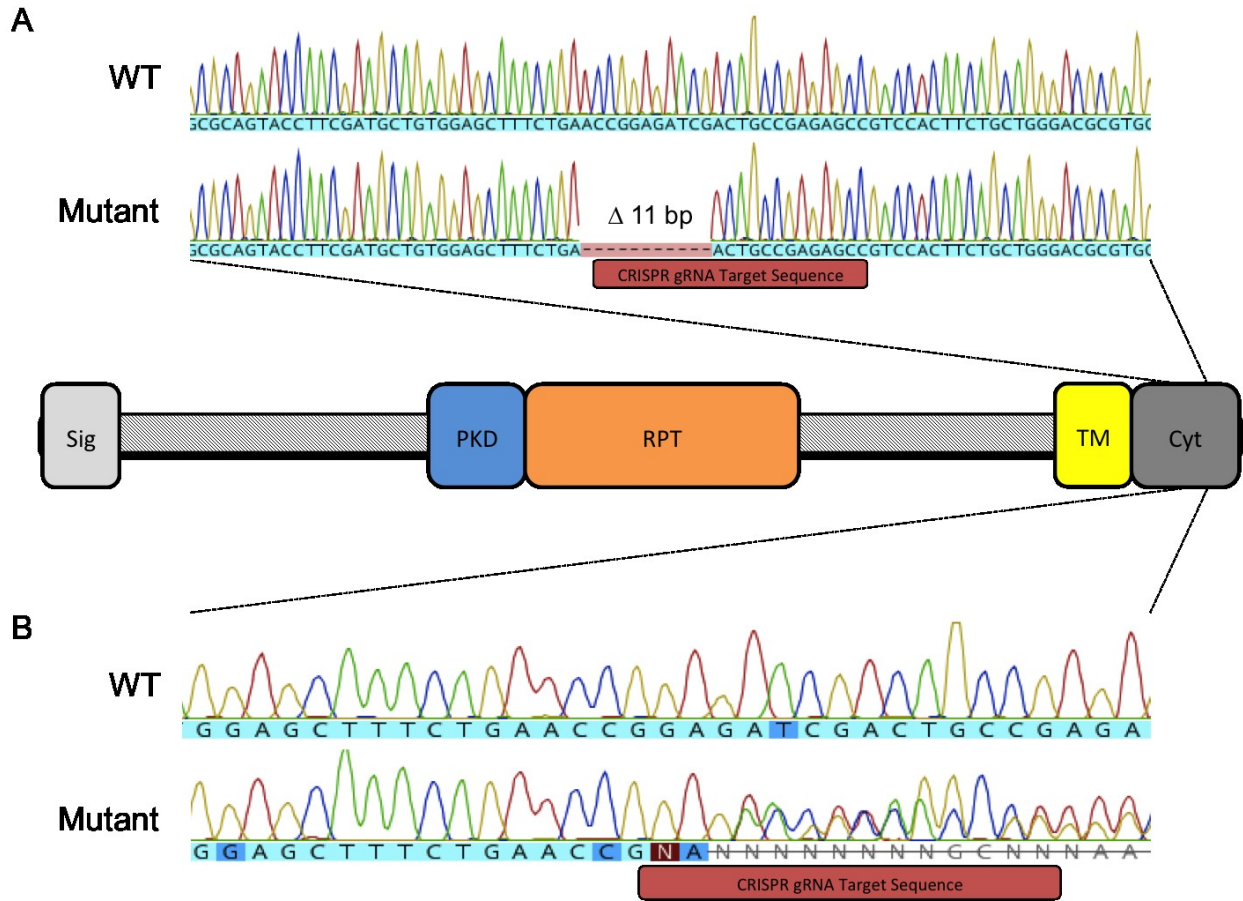
Figure 17: The sequencing information of adult pmela *stable mutants[37].*
A) *An 11 base pair (bp) deletion in the cytoplasmic region of* pmela *in an adult zebrafish. Transcript was from TA TOPO cloned individual. B) A heterozygous 1 bp deletion in the cytoplasmic region of* pmela *in an adult zebrafish. Transcript was from direct sequencing of PCR product from whole DNA extract.*

3.3 Zebrafish Homozygous for Allele ua5022 Have Pigment and Ocular Defects

Heterozygous ua5022 zebrafish did not present with any abnormal phenotypes as larvae or as adults. When heterozygote ua5022 zebrafish were bred with each other, the offspring presented with a 3:1 ratio of wild type to mutant pigment phenotypes, indicating a potential mechanism of recessive Mendelian inheritance. Phenotypically the mutants presented with globally reduced pigment. Several individuals from the phenotypically mutant and wild type groups were sequenced. It was determined that all individuals with the abnormal phenotype were homozygous for the ua5022 allele. No phenotypically wild type individuals were homozygous for the mutation, which allowed for the identification of homozygous ua5022 mutants via their phenotype.

At 3 dpf, homozygous ua5022 zebrafish larvae were observed to have a global pigment reduction phenotype and no abnormal ocular phenotypes (Figure 18a,b). This phenotype closely resembles the phenotype that is seen in the *pmela* morphants, and validates what was seen in the morphant data. In morphants, the persistence of the pigment reduction phenotype past 3 dpf could not be observed, presumably due to MO degradation. In ua5022 fish, this was no longer a limitation. We observed at 6 dpf that the global pigment reduction phenotype persisted and was more pronounced than at 3 dpf; the pigment globally was reduced and appeared more vein like, while the pigment in the eyes was also reduced and looked more patch-like in nature (Figure 18c,d). No abnormal ocular structural phenotype was observed at this stage (Figure 18c,d).
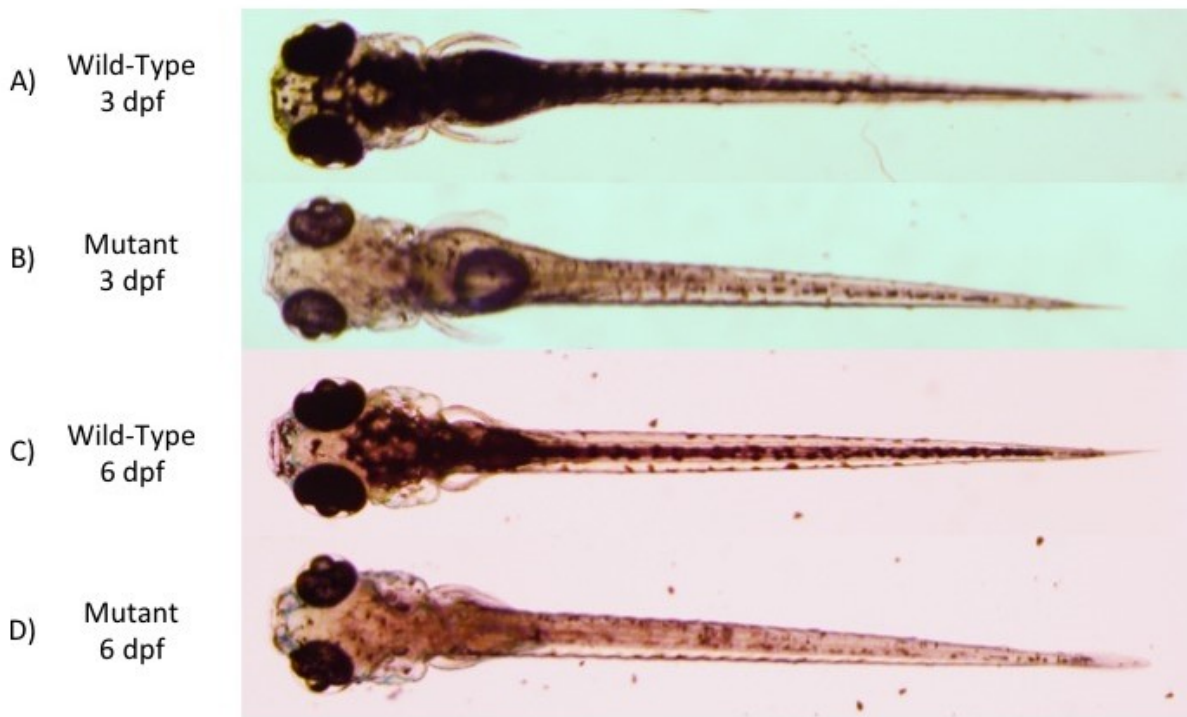
Figure 18: Wild type and mutant ua5022 zebrafish at 3 days post fertilization and 6 days post fertilization[37].

A) A representative phenotypically wild type zebrafish at 3 days post fertilization (dpf). *B)* A representative mutant ua5022 zebrafish at 3 dpf. Global pigment reduction is apparent, but ocular structural abnormalities are not apparent. *C)* A representative phenotypically wild type zebrafish at 6 dpf. *D)* A representative mutant ua5022 zebrafish at 6 dpf. Global reduction is observed to have increased since 3 dpf. Ocular structural abnormalities are still not apparent.

An overt abnormal structural ocular phenotype is first observed in the homozygous ua5022 larvae at 8 dpf (Figure 19b,d). At this age, the mutant larvae have significantly reduced pigmentation (p<0.001) compared to their phenotypically wild type siblings (Figure 19a, Figure 20a). When measured, it was found that compared to body length, the length of the eye (p<0.001) (Figure 20c) and the perimeter of the eye (p<0.001) (Figure 20d) of homozygous ua5022 zebrafish were significantly smaller than their phenotypically wild type siblings, indicating that the mutants have microophthalmia, smaller eyes. The size of the anterior chamber, measured as the space between the cornea and the lens, was significantly higher (p<0.001) in the homozygous mutants (Figure 20e). Additionally, it was determined that the eyes of the homozygous mutants did not have a normal shape. The shape was measured by taking the circumference of the eye and dividing it by the length of the eye; this measurement was significantly (p<0.001) different for the mutants (Figure 20f).
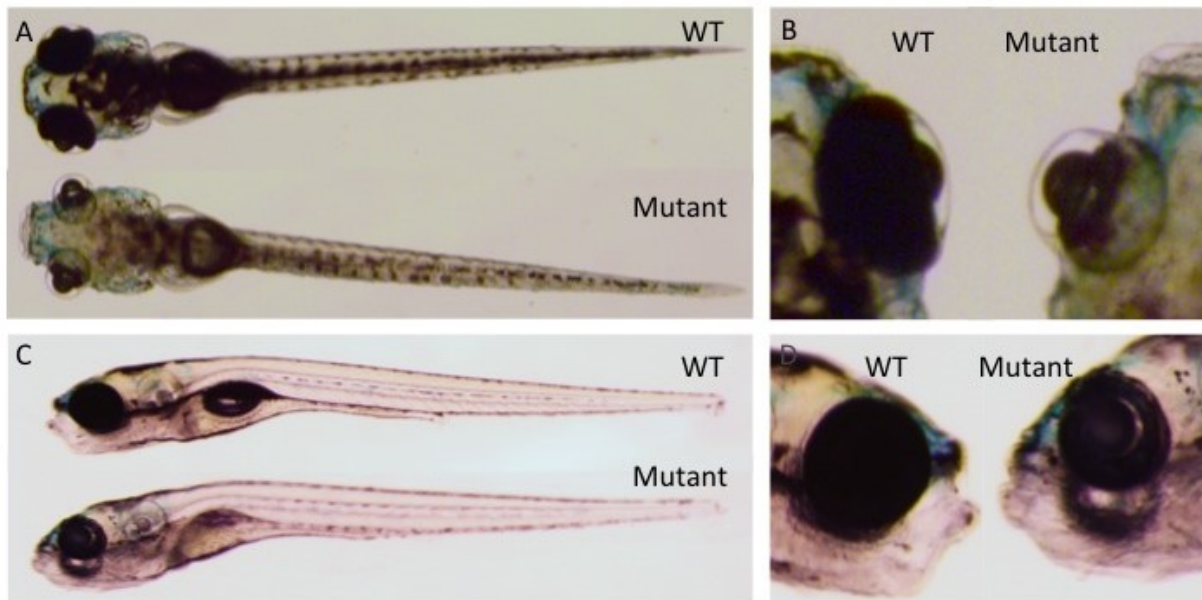
Figure 19: Mutant ua5022 zebrafish at 8 days post fertilization have global pigment reduction and ocular abnormalities[37].
*A) Phenotypically wild type (WT) and ua5022 mutant 8 days post fertilization zebrafish from a dorsal view showing apparent global pigment reduction. **B)** A close up dorsal view of the eyes of WT and mutant ua5022 zebrafish at 8 dpf showing apparent abnormalities in ocular structure in mutant zebrafish, most notably a distended anterior segment. **C)** Lateral view of whole WT and mutant zebrafish at 8 dpf. **D)** A close up lateral view of the eyes of WT and mutant ua5022 zebrafish at 8 dpf.*
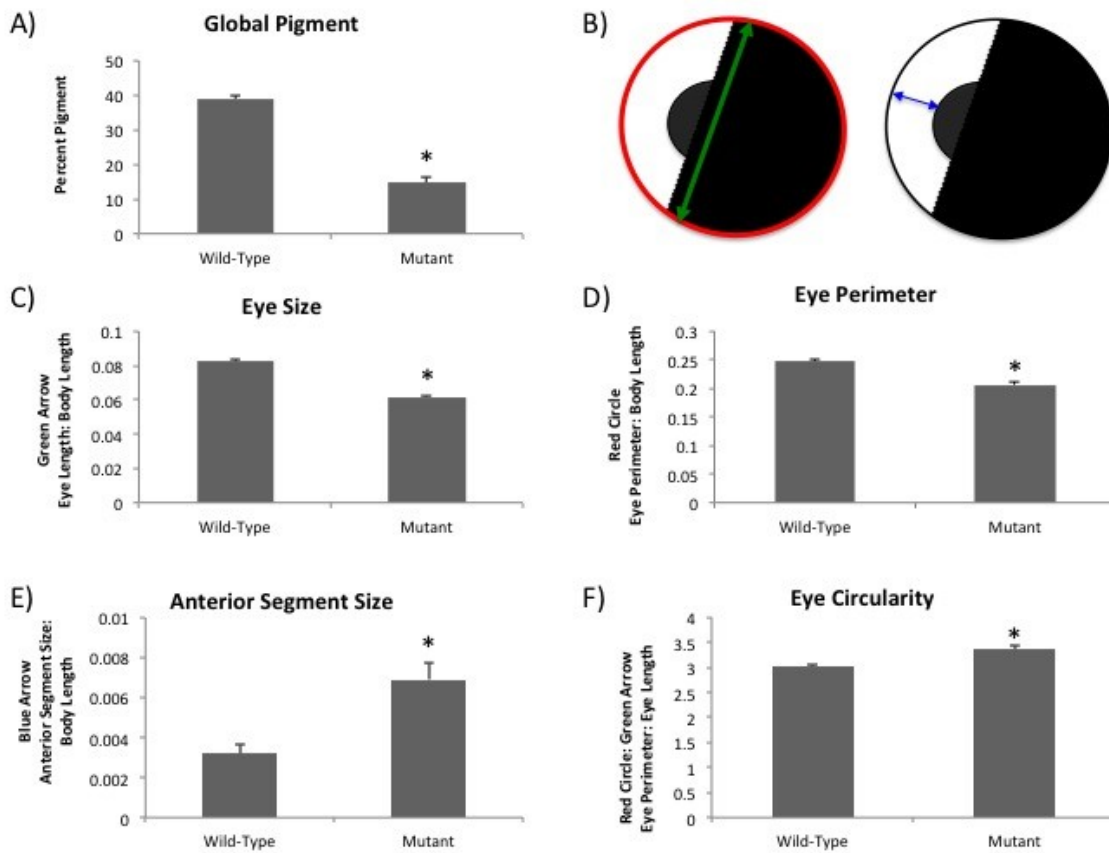
Figure 20: Significant reduction in global pigment, reduction in eye size, increase in anterior segment size, and change in eye shape in ua5022 mutants[37].
Wild-type, n=14, Mutant, n=3. Siblings. Error bars: Standard Error A) Homozygous ua5022 zebrafish have significantly (p<0.001) less pigmentation than sibling phenotypically wild type zebrafish. B) A schematic detailing how eye size (green arrow), eye perimeter (red circle) and anterior segment size (blue arrow) were measured. C) The length of homozygous ua5022 zebrafish eyes in ratio to body length were significantly (p<0.001) smaller than in phenotypically wild type siblings. D) The perimeter of homozygous ua5022 zebrafish eyes in ratio to body length were significantly (p<0.001) smaller than in phenotypically wild type siblings. E) The anterior segment size of homozygous ua5022 zebrafish eyes in ratio to body length was significantly (p<0.001) larger than in phenotypically wild type siblings. F) The circularity of the homozygous ua5022 eyes, as was calculated by taking the ratio of the perimeter of the eye and dividing it by the length of the eye, were significantly different from the circularity of the wild type sibling eyes.

When homozygous ua5022 larvae were analyzed via qPCR for their relative abundances of *pmela* mRNA and *pmelb* mRNA, it was found that compared to wild type, non-sibling zebrafish the levels of *pmela* ($p<0.001$) (Figure 21a) and *pmelb* ($p<0.001$) (Figure 21b) were significantly reduced by over 20-fold in ua5022 homozygotes.
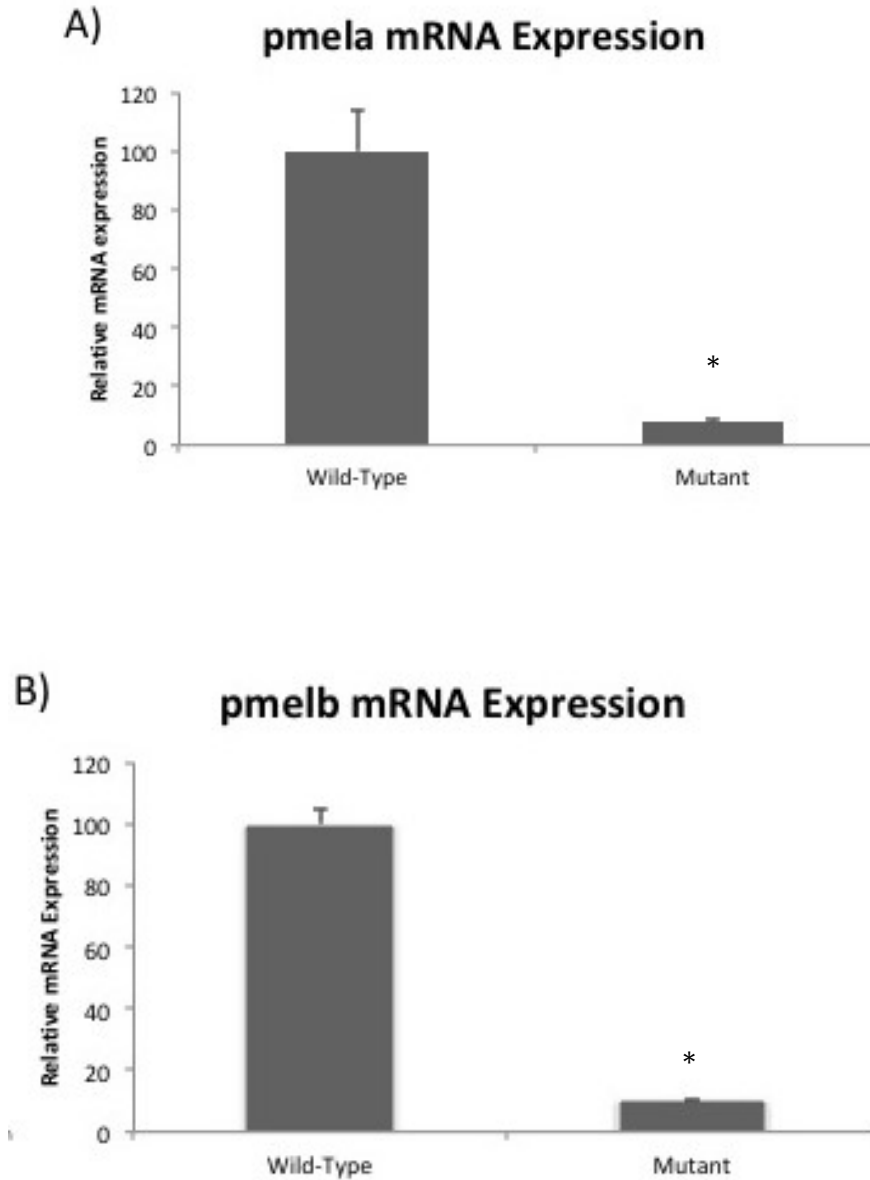
Figure 21: Homozygous ua5022 mutants have reduced pmela *and* pmelb *mRNA transcript levels[37].*

*Wild-type, n=5. Mutant, n=5, 3 replicates each. **A)** The expression of* pmela *mRNA transcripts was significantly (p<0.001) reduced by almost 20-fold in 3 days post fertilization homozygous ua5022 mutants compared to wild type non-sibling zebrafish. β-actin was used as a reference.* ***B)** The expression of* pmelb *mRNA transcripts was significantly (p<0.001) reduced by approximately 10 fold in 3 days post fertilization homozygous ua5022 mutants compared to wild type non-silbing zebrafish. β-actin was used as a reference.*

Several homozygous ua5022 larvae were analyzed for mutations in the C-terminal region of *pmelb* to see if there was any non-specific targeting of the gene by the CRISPR sequence that would result in the reduction of *pmelb* mRNA transcripts. No mutations were found in the last three exons of *pmelb* in any of the individual larvae that were analyzed.

We attempted to grow some of the homozygous ua5022 individuals to adulthood. Currently, some individuals have survived beyond the larval stage, but are developmentally delayed, appearing to still be in the juvenile stage even after over two months has passed since fertilization.

3.4 Zebrafish with Allele ua5021 Do Not Have Overt Pigment Phenotypes

Heterozygous ua5021 zebrafish did not present with any abnormal phenotypes as larvae or as adults. Unlike with the ua5022 allele, when the heterozygous ua5021 zebrafish were bred with each other, there was no easily identifiable phenotype present in any of the offspring. It was not until 12 dpf that some individuals became less pigmented than others and those same individuals began to develop an enlarged anterior segment. However, due to problems with DNA processing homozygote mutants larvae could not be confirmed. All offspring of the heterozygote ua5021 zebrafish cross were raised to adulthood.

Chapter 4: Discussion

Portions of this chapter were written for "Non-Synonymous variants in Premelanosome Protein (PMEL) cause ocular pigment dispersion and pigmentary glaucoma." Adrian A. Lahola-Chomiak *et al.* (Submitted)

4.1 Homozygous *pmela* ua5022 Zebrafish have PG/PDS Associated Phenotypes

In experiments done by our collaborators (the Walter lab), they used a cell model and the patient variants of PMEL to elucidate PMEL's role in PG/PDS. Through these studies, they were able to determine that, on a cellular level, patient variants in PMEL cause defects in proper PMEL protein processing, and pseudomelanosome structure[37]. However, these *in vitro* experiments were not able to give us insight into PG/PDS beyond the cellular level. In order to better understand the effect of deficits in PMEL, we developed an animal model. An animal model allowed us to observe the effect of mutant PMEL on cellular function as well as tissue, organ, and system function and organization.

To examine how mutations in PMEL affect the interactions between cells and affect whole systems, we created a zebrafish animal model. Using our animal system, we can more clearly model disease progression as seen in humans. By understanding the mechanisms underlying PG/PDS we may be able to find other candidate genes that are causative of the disease.

There were many advantages in creating a zebrafish animal model over working in other animal model systems. Advantages of using zebrafish include short development time to sexual maturity, external fertilization, and well-characterized genetic tools[73, 74]. The zebrafish has an ocular system that accurately models the human ocular system[73-75, 77, 79].

We were able to look for the lack of pigment phenotype in the knockout fish based upon previous MO work done[67, 70] and our own observations with MOs as an initial confirmation of our knock out model.

We initially chose seven CRISPR sites to target in *pmela*. All sites were predicted to have high fidelity and minimal off target affects. Of these, only one CRISPR sequence was found to produce mutations. The CRISPR that produced the mutation was targeted to the CYT region. Notably, the majority of PMEL mutations that cause pigment and ocular defects in other species are within this region[59-63, 65, 66]. However, only one identified human patient mutation is localized within the CYT region. Future work will look at targeting other regions within the *pmela* gene to examine whether mutations in these regions also result in measurable phenotypes. The RPT region, where most the patient mutations are found, would be the first target for further study.

In the ua5022 mutant model, we observed changes in global pigmentation and changes in ocular morphology. Similar to our observations in MO injections, zebrafish homozygous for the ua5022 allele have reduced pigmentation that can be observed from 3 dpf. In addition, at 8 dpf, the ocular morphology of the zebrafish larvae shows expansion of the anterior segment and altered ocular shape. These observations support the presence of high intraocular pressure. High intraocular pressure would explain the changing of eye shape, which can result in a more spherical configuration and explains the pushing of the cornea away from the lens. However, in order to confirm that we have made a glaucoma model, we will need to look at the health of the RGCs. Previous zebrafish models of high intraocular pressure have been associated with RGC death [89].

Currently, we have characterized the global pigmentation and the ocular structure of homozygous mutant ua5022 larvae. In order to better understand the effects of this mutation, we will need to further characterize the phenotype of these larvae by looking at

specific cells types in the eyes. This can be achieved by sectioning the eye, immunofluorescence, and fluorescence microscopy. It will also be important to observe the structure of the melanosomes in the different pigmented structures of the eye, specifically the iris and the RPE, and compare mutant melanosomes to wild type melanosomes. We would expect differences in melanosome structure, because of the experimental work that was performed in our collaborator's *in vitro* assays[37] as well as the changes observed in melanosome shape in mutant PMEL chickens, zebrafish, and mice[64, 67, 69, 70].

Our homozygous mutants have been observed to grow to the juvenile stage. This means that there is a potential that we will be able to observe the effect of *pmela* knock out in adulthood. After further characterizing the ua5022 homozygotes as larvae, it will be important to characterize them as adults. This would involve the characterization of the global pigment of the adults, the ocular structure, the RGCs, and the melanosomes. In our knock out zebrafish, we will be able to observe how these mutations affect the ocular system over the life span of an animal. It is important to keep track of the progression of the phenotype over the lifetime of the animal because many causes of PG/PDS are observed later in life in humans.

By creating a knock out model of an ortholog of PMEL, we now have an *in vivo* system to test patient mutations. These experiments can be used to support and confirm the observations from the *in vitro* experiments[37]. To confirm patient mutation pathogenicity, we would have to introduce these variants of PMEL into homozygous mutant ua5022 embryos. We would then observe how the introduction of the patient variants affects the development of zebrafish ocular structure and pigmentation compared

79

to wild type zebrafish, zebrafish mutants that have had wild type PMEL reintroduced, and zebrafish mutants who have an unrelated control gene introduced.

Through the PMEL animal model, we can gain further insight into the dysfunctional vs. mechanical debate of how pigment sloughs off of the iris[24, 28]. The dysfunctional school of thought believes that pigment sloughs off the iris due to aberrant function of the pigmented cells of the iris; the structural school of though believes that pigment is sloughed off the iris through the mechanical rubbing of altered structures such as the bowing of the zonules. With the discovery of PMEL as a candidate gene, we give credence to the dysfunctional hypothesis due to PMEL's role in melanosome function and health. However, we can also attempt to find any structural differences that are caused by the mutation that would exacerbate the phenotype through physical contact with pigmented structures. We can look for pigment in the aqueous humor and the deposition of pigment on the annular ligament in the zebrafish eye and correlate the severity of pigment sloughing or capture to the severity of the disease.

Currently we have only characterized ua5022 homozygous mutants. Heterozygote ua5022 fish will have to be characterized to see if they also have any larval or adult onset phenotypes. The characterization of heterozygotes may more accurately model the PG/PDS disease phenotype in humans. The human phenotype is not as severe as what is observed in our homozygous mutants. PG/PDS has not been associated with reduction in pigment of any other organs except the eye in humans, but we see global pigment reduction in our homozygous fish. Our other *pmela* mutant, which does not display such overt pigment phenotypes, may model the disease phenotypes we see in human PG/PDS.

4.2 The Difference Between the ua5022 and ua5021 Mutants

We were able to create two different *pmela* mutants using one CRISPR gRNA. The 11-bp deletion of the ua5022 allele causes the deletion of 3 amino acids and a frame shift of two nucleic acids, which is expected to extend the size of the protein by 79 amino acids. The 1 bp- deletion of the ua5021 allele causes a frame shift of one amino acid, which theoretically would extend the size of the protein by 17 amino acids.

Both mutations were predicted to have sizeable effects at the protein level, causing frameshifts that would theoretically extend the protein considerably, and we expected that both of the mutant lines would have large impacts on observed phenotypes. When we characterized homozygous ua5022 mutants, we observed a phenotype at 3 dpf and that this phenotype progressed with age. We determined that the observed phenotype was due to the non-sense mediated decay of *pmela* transcripts[130-132]. This finding supports our hypothesis that loss of pmela is what underlies the phenotype. We expected that when we characterized the ua5021 line that we would see the same results. However, apparent abnormal phenotypes were not observed in the ua5021 line until a much later stage.

This phenotypic difference indicates that the two mutations have different functional consequences. The ua5022 mutation has a greater functional impact when compared to the ua5021 line. In order to better characterize these differences, the ua5021 heterozygous cross offspring will have to be phenotyped and individually sequenced. It will be important to characterize this line in their larval and adult stages in both the homozygous and heterozygous mutant forms.

There are a couple different reasons why there could be phenotypic differences between the ua5022 line and the ua5021 line. The phenotypic differences could be due to

the mRNA transcripts in the ua5021 line not undergoing non-sense mediated decay like the ua5022 transcripts. All transcripts would be available for translation and the appropriate amount of pmela protein made. Because a subtle phenotype was observed at 12 dpf, it is likely that this protein lost some of its function. Alternatively, in the ua5021 line there may have been some non-sense mediated decay, but not to the extent of the ua5022 line resulting in fewer transcripts available for translation and less protein made. In this mechanism, there may not have been enough functional protein produced and/or the protein has lost some function due to the placement and size of the mutation at the C-terminus of the protein. A threshold mechanism of disease burden would then account for the phenotype being observed at a later time. This would implicate the dysfunctional school of thought, being that the death of pigment cells would only come after the accumulation of enough mutant protein.

We were not able to run qPCR on the ua5021 line, because homozygous mutants were not readily identifiable due to the lack of a genotype/phenotype correlation that was overt in the ua5022 line. Currently we are unable to confirm the underlying mechanism resulting in the observed phenotype differences.

To elucidate the reason for why the two mutations function differently we would first have to identify ua5021 homozygous mutant individuals through the sequencing of the C-terminus of *pmela* in individual larvae. We would then perform qPCR to detect *pmela* transcript levels.

If *pmela* mRNA levels were equivalent to wild type levels of *pmela* mRNA, the next step would be to discern if the protein is translated. We would have to design an antibody that would be able to detect pmela. An antibody would be used for both western blotting to

check for the presence of protein and for immunofluorescence microscopy to detect if pmela is being processed and transported properly in the cell. If an antibody cannot be designed to detect pmela, then we would be to observe the ultrastructure of melanosomes to see if the mutant pmela changes the organelle or fibril structure. We would expect that the shape of the melanosomes would be circular and that the fibril structure would be disorganized[37].

If *pmela* mRNA levels in ua5021 homozygous mutants were significantly lower than wild type levels, but significantly higher than in ua5022 homozygous mutants, then we would determine if there is a similar pattern in the protein levels. This would require an antibody to measure protein levels and detect if there are any trafficking defects with the protein, which may be causative of an intermediate phenotype. In the absence of an antibody, the ultrastructure of melanosomes can be observed to look for abnormalities, especially compared to the melanosomes of ua5022 mutants.

If the *pmela* mRNA transcript levels in ua5021 mutants are very low as in the ua5022 mutants, then we would have to consider the possibility of compensation of pmela function by related proteins, namely pmelb.

4.3 The Implication of the Reduction of *pmelb* in *pmela* Mutants

In the characterization of the ua5022 line we also discovered that there was a reduction in *pmelb* mRNA transcripts; this was unexpected. It is likely that the reduced mRNA levels resulted from the lack of transcription of the *pmelb* gene rather than non-sense mediated decay. In addition, there was no evidence to suggest that there were any mutations in the C-terminal region of *pmelb* that would result in non-sense mediated decay[130-132].

If *pmelb* was never transcribed, this supports the idea that pmela activates the transcription of *pmelb*. This relationship has never before been implied in the literature. This finding may have several implications for the mechanism of function of PMEL in zebrafish.

If the knock out of *pmela* also results in the loss of *pmelb*, pmelb is not compensating for the loss of pmela. This means that pmelb may not have a role in compensating pmela lack of function. Pmelb may have its own unique function within the cell. This function may be independent or dependent on the presence of *pmela*. This is supported by previous *in situ* analysis, which have localized *pmelb* to different structures in the zebrafish compared to *pmela[67, 133-136]*. It is possible that pmelb does not have a function that is related to melanosome development and pigmentation. There is currently the lack of phenotypic evidence to support this conjecture. However, the fact that no abnormal pigment phenotypes have been associated with the loss of pmelb may indicate a separate function for pmelb. This is supported by the *in situ* hybridizations that localize *pmelb* to only the RPE and no other pigmented structures in embryos[67, 133, 136]. These findings also imply that the pmelb function may be retained in PMEL orthologs that have not had a genome duplication.

The reduction of *pmelb* in *pmela* ua5022 homozygous mutants also convolutes our conclusion that *pmela* is a major player in pigmentation and ocular functioning. Due to the reduction of both gene transcripts in the ua5022 homozygotes, we cannot conclude that the effect of the loss of *pmela* is alone the cause of the observed phenotype. It is possible that the loss of one gene is responsible for one phenotype, for example the loss of *pmela* causing

the loss of pigmentation, while the loss of the other gene causes the other phenotype, such as the loss of *pmelb* causing the ocular abnormalities.

The role of pmela and pmelb in these phenotypes may be better characterized in the ua5021 homozygotes. The relative levels of *pmelb* mRNA is currently unknown in these mutants, which have a slightly altered phenotype. By measuring the *pmelb* mRNA levels in homozygous mutants we can further analyze the effect of pmelb on pigmentation and ocular structure.

We can also approach the question of pmelb functionality and how it interacts with pmela by creating a *pmelb* knock out model with CRISPR/Cas9. A knock out line may allow us to answer the questions that *pmelb* MO work has currently not been able to. The creation of this model may allow for us to directly observe the effects of the loss of pmelb alone, and therefore also potentially test pmelb's role in creating PG/PDS-like symptoms.

Both *pmela* and *pmelb* are orthologs of the single copy of human PMEL. This means that the effects due to the loss of either of these genes can be correlated to effects seen when human PMEL is mutated.

4.4 PMEL as a Candidate Gene for PG/PDS

Prior to the work of our colleagues, PG/PDS was not associated with a gene; although, it has long been thought that the disease is hereditary[26, 31]. In this study, we mutated a zebrafish homolog of PMEL and observed phenotypes that could be associated seen in PG. These findings support the theory that there is a dysfunctional component involved in the progress of PG/PDS. Whether or not there is also a structural or an environmental component to the development of these phenotypes will have to be explored. Future work could include the observation of the zonules, which are the

structures that is thought to cause the sloughing of pigment from the iris in PG/PDS in the structural model [24-26, 34]. If we observe these structures in the mutant zebrafish, we might be able to develop a combined theory as to how PG develops [26].

In discovering that PMEL is a gene associated with PG, we can begin to explain the mechanism by which PG can generally develop. As well, we can identify other genes that might be at play in those who suffer from the disease but have no mutations in PMEL.

Identifying mutations in PMEL that lead to PG may mean that we will be able to come up with better diagnostic tools that are related to PMEL deregulation. By diagnosing the disease earlier, blindness can be prevented or slowed for the patient through improved treatment options. This is extremely important in families with a history of PG/PDS, so that they can be counseled and are aware of the care they may need to have if they have a genetic predisposition to the disease. Approved treatments can begin to be developed by addressing the dysfunction that is caused when PMEL is disrupted, of which could also be the same or similar dysfunction in non-PMEL associated cases of PG.

Experiments that would be able to help us further understand the mechanism of PMEL in PG would involve the detection of pigment granules in the anterior segment of the zebrafish eye and how the composition of these pigment granules may change in their deposition over time. It has been mentioned that many of the symptoms of PG/PDS are transitory, making it hard to diagnose the disease. Understanding how the levels of these pigment granules change, and what conditions can cause them to build up on the cornea or in the trabecular meshwork would be able to help us better understand, diagnose, and treat the disease. We could determine if there is a correlation between pigment reduction and the buildup of pigment in the different ocular structures and fluids. We can also document

how aqueous humor outflow changes with the severity of the disease phenotype, developmental stage of the zebrafish, or presence of the current symptoms. We could test to see the rate of outflow of the aqueous humor in different mutant configurations, or with various potentially transitory phenotypes present. We could then also detect if the aqueous humor outflow is correlated to the intraocular pressure of the zebrafish eye and the health of the RGCs.

4.6 Conclusions

In our study, we supported the identification of PMEL as a candidate gene for PG. In *in vitro* tests, our collaborators were able to demonstrate that patient variants of PMEL can change the normal processing of the protein and alter the structure of the organelle in which PMEL functions, the melanosomes[37]. We believed that melanosomes played a large role in the progress of this disease, and these findings supported that patient mutations of PMEL alter the proper functioning of these melanosomes.

To further implicate PMEL in PG disease pathology, we created a zebrafish animal model that would allow us to model PMEL mutations and observe ocular abnormalities. In knocking down and knocking out a PMEL ortholog, we displayed how the dysfunction or loss of this protein can directly influence ocular structure. The combination of the *in vitro* experimental work and this *in vivo* study supports PMEL's role in the progression of PG.

By providing more evidence for this first candidate gene, we will be able to better identify other genes that may be involved in PG/PDS, elucidate the mechanism of this disease, develop better diagnostic tools and novel treatment avenues.

Bibliography:

1. Ort, V.H., D. *Development of the Eye*.
2. Yang, J.P., C; Bindra, S; Rastogi, A; Banergee, T; Gupta, Y, *Vision Facts: Questions about the Human Eye*. 2018, USA: Universal Publishers, Inc.
3. *Retinal Development*, ed. E.E. Sernagor, S; Harris, B; Wong, R. 2006: Cambridge University Press.
4. Felten, D.L.O.B., M.K; Maida, M.S, *Netter's Atlas of Neuroscience*. 2016.
5. Goel, M., et al., *Aqueous humor dynamics: a review.* Open Ophthalmol J, 2010. **4**: p. 52-9.
6. Kevany, B.M. and K. Palczewski, *Phagocytosis of retinal rod and cone photoreceptors.* Physiology (Bethesda), 2010. **25**(1): p. 8-15.
7. Selhorst, J.B. and Y. Chen, *The optic nerve.* Semin Neurol, 2009. **29**(1): p. 29-35.
8. Tham, Y.C., et al., *Global prevalence of glaucoma and projections of glaucoma burden through 2040: a systematic review and meta-analysis.* Ophthalmology, 2014. **121**(11): p. 2081-90.
9. Jonas, J.B., et al., *Glaucoma.* The Lancet, 2017. **390**(10108): p. 2183-2193.
10. Friedman, J.S.W., M.A., *Glaucoma genetics, present and future.* Clin Genet, 1999. **55**: p. 71-79.
11. Challa, P., *Glaucoma genetics.* Int Ophthalmol Clin, 2008. **48**(4): p. 73-94.
12. Quigley, H.A., *Neuronal death in glaucoma.* Progress in Retinal and Eye Research, 1999. **18**(1): p. 39-57.
13. Kerrigan, L.A.Q., H.A.; Pease, M.E.; Kerrigan, D.F.; Mitchell, R.S., *Number of Ganglion Cells in Glaucoma Eyes Compared with Threshold Visual Field Tests in the Same Persons.* Invest. Ophthalmol. Vis. Sci, 2000. **41**: p. 741-748.
14. Nickells, R.W., *Retinal ganglion cell death in glaucoma: the how, the why, and the maybe.* J Glaucoma, 1996. **5**(5): p. 345-356.
15. Liu, Y. and R.R. Allingham, *Molecular genetics in glaucoma.* Experimental Eye Research, 2011. **93**(4): p. 331-339.
16. Gemenetzi, M., Y. Yang, and A.J. Lotery, *Current concepts on primary open-angle glaucoma genetics: a contribution to disease pathophysiology and future treatment.* Eye (Lond), 2012. **26**(3): p. 355-69.
17. Leske, M.C., *The Epidemiology of Open-Angle Glaucoma: A Review.* American Journal of Epidemiology, 1983. **118**(2): p. 166-191.
18. Quigley, H.A. and A.T. Broman, *The number of people with glaucoma worldwide in 2010 and 2020.* Br J Ophthalmol, 2006. **90**(3): p. 262-7.
19. Abu-Amero, K., A. Kondkar, and K. Chalam, *An Updated Review on the Genetics of Primary Open Angle Glaucoma.* International Journal of Molecular Sciences, 2015. **16**(12): p. 28886-28911.
20. Tielsch, J.M., *Racial Variations in the Prevalence of Primary Open-angle Glaucoma.* Jama, 1991. **266**(3).
21. Sommer, A., *Intraocular Pressure and Glaucoma.* American Journal of Ophthalmology, 1989. **107**(2): p. 186-188.
22. *Natural history of normal-tension glaucoma.* Ophthalmology, 2001. **108**(2): p. 247-253.

23. Quigley, H.A., *Optic Nerve Damage in Human Glaucoma.* Archives of Ophthalmology, 1981. **99**(4).

24. Lahola-Chomiak, A.A. and M.A. Walter, *Molecular Genetics of Pigment Dispersion Syndrome and Pigmentary Glaucoma: New Insights into Mechanisms.* J Ophthalmol, 2018. **2018**: p. 5926906.

25. Campbell, D.G., *Pigmentary Dispersion and Glaucoma.* Archives of Ophthalmology, 1979. **97**(9).

26. Farrar, S.M. and M.B. Shields, *Current concepts in pigmentary glaucoma.* Survey of Ophthalmology, 1993. **37**(4): p. 233-252.

27. Richter, C.U., *Pigmentary Dispersion Syndrome and Pigmentary Glaucoma.* Archives of Ophthalmology, 1986. **104**(2).

28. Niyadurupola, N. and D.C. Broadway, *Pigment dispersion syndrome and pigmentary glaucoma - a major review.* Clinical & Experimental Ophthalmology, 2008. **36**(9): p. 868-882.

29. Migliazzo, C.V., et al., *Long-term Analysis of Pigmentary Dispersion Syndrome and Piegmentary Glaucoma.* Ophthalmology, 1986. **93**(12): p. 1528-1536.

30. Speakman, J.S., *Pigmentary dispersion.* British Journal of Ophthalmology, 1981. **65**(4): p. 249-251.

31. Siddiqui, Y., et al., *What is the risk of developing pigmentary glaucoma from pigment dispersion syndrome?* American Journal of Ophthalmology, 2003. **135**(6): p. 794-799.

32. Lascaratos, G., A. Shah, and D.F. Garway-Heath, *The genetics of pigment dispersion syndrome and pigmentary glaucoma.* Surv Ophthalmol, 2013. **58**(2): p. 164-75.

33. Bick, M.W., *Pigmentary Glaucoma in Females.* Archives of Ophthalmology, 1957. **58**(4): p. 483-494.

34. Campbell, D.G.S., R.M., *Pathophysiology of pigment dispersion syndrome and pigmentary glaucoma.* Current Opinion in Ophthalmology, 1995. **6**(2): p. 96-101.

35. Scheie, H.G.F., H.W., *Idiopathic Atrophy of the Epithelial Layers of the Iris and Ciliary Body.* Trans. Am. Ophthalmol. Soc., 1957. **55**: p. 369-391.

36. Sowka, J., *Pigment dispersion syndrome and pigmentary glaucoma.* Optometry - Journal of the American Optometric Association, 2004. **75**(2): p. 115-122.

37. Lahola-Chomiak, A.A., *Non-Synonymous Variants in the Premelanosome Protein (PMEL) Gene are Associated with Pigment Dispersion Syndrome/Pigmentary Glaucoma and Cause Biochemical Defects*, in *Medical Genetics*. 2018, University of Alberta.

38. Bissig, C., L. Rochin, and G. van Niel, *PMEL Amyloid Fibril Formation: The Bright Steps of Pigmentation.* Int J Mol Sci, 2016. **17**(9).

39. Watt, B., et al., *PMEL: a pigment cell-specific model for functional amyloid formation.* Pigment Cell Melanoma Res, 2013. **26**(3): p. 300-15.

40. Fowler, D.M., et al., *Functional amyloid formation within mammalian tissue.* PLoS Biol, 2006. **4**(1): p. e6.

41. Theos, A.C., et al., *A lumenal domain-dependent pathway for sorting to intralumenal vesicles of multivesicular endosomes involved in organelle morphogenesis.* Dev Cell, 2006. **10**(3): p. 343-54.

42. Leonhardt, R.M., et al., *Critical residues in the PMEL/Pmel17 N-terminus direct the hierarchical assembly of melanosomal fibrils.* Mol Biol Cell, 2013. **24**(7): p. 964-81.

43.   Hee, J.S., et al., *Melanosomal formation of PMEL core amyloid is driven by aromatic residues.* Sci Rep, 2017. **7**: p. 44064.
44.   Watt, B., et al., *N-terminal domains elicit formation of functional Pmel17 amyloid fibrils.* J Biol Chem, 2009. **284**(51): p. 35543-55.
45.   Hoashi, T., et al., *The Repeat Domain of the Melanosomal Matrix Protein PMEL17/GP100 Is Required for the Formation of Organellar Fibers.* Journal of Biological Chemistry, 2006. **281**(30): p. 21198-21208.
46.   McGlinchey, R.P., et al., *The repeat domain of the melanosome fibril protein Pmel17 forms the amyloid core promoting melanin synthesis.* Proc Natl Acad Sci U S A, 2009. **106**(33): p. 13731-6.
47.   Pfefferkorn, C.M., R.P. McGlinchey, and J.C. Lee, *Effects of pH on aggregation kinetics of the repeat domain of a functional amyloid, Pmel17.* Proc Natl Acad Sci U S A, 2010. **107**(50): p. 21447-52.
48.   Ancans, J., et al., *Melanosomal pH Controls Rate of Melanogenesis, Eumelanin/Phaeomelanin Ratio and Melanosome Maturation in Melanocytes and Melanoma Cells.* Experimental Cell Research, 2001. **268**(1): p. 26-35.
49.   Ho, T., et al., *The Kringle-like Domain Facilitates Post-endoplasmic Reticulum Changes to Premelanosome Protein (PMEL) Oligomerization and Disulfide Bond Configuration and Promotes Amyloid Formation.* Journal of Biological Chemistry, 2016. **291**(7): p. 3595-3612.
50.   Watt, B., et al., *Mutations in or near the transmembrane domain alter PMEL amyloid formation from functional to pathogenic.* PLoS Genet, 2011. **7**(9): p. e1002286.
51.   Theos, A.C., et al., *Dual loss of ER export and endocytic signals with altered melanosome morphology in the silver mutation of Pmel17.* Mol Biol Cell, 2006. **17**(8): p. 3598-612.
52.   Allison, W., et al., *Reduced Abundance and Subverted Functions of Proteins in Prion-Like Diseases: Gained Functions Fascinate but Lost Functions Affect Aetiology.* International Journal of Molecular Sciences, 2017. **18**(10).
53.   Maury, C.P., *The emerging concept of functional amyloid.* J Intern Med, 2009. **265**(3): p. 329-34.
54.   Jackson, M.P. and E.W. Hewitt, *Why are Functional Amyloids Non-Toxic in Humans?* Biomolecules, 2017. **7**(4).
55.   Rambaran, R.N.S., L.C., *Amyloid Fibrils.* Prion, 2008. **2**(3): p. 112-117.
56.   Kitamoto, T., et al., *Amyloid plaques in Creutzfeldt-Jakob disease stain with prion protein antibodies.* Ann Neurol, 1986. **20**(2): p. 204-8.
57.   Medori, R., et al., *Fatal familial insomnia, a prion disease with a mutation at codon 178 of the prion protein gene.* N Engl J Med, 1992. **326**(7): p. 444-9.
58.   Rochin, L., et al., *BACE2 processes PMEL to form the melanosome amyloid matrix in pigment cells.* Proc Natl Acad Sci U S A, 2013. **110**(26): p. 10658-63.
59.   Hecht, B.C., *Sequence Analysis of PMEL17 as Candidate Gene for Causing Rat-Tail Syndrome in Cattle*. 2006, Brigham Young University.
60.   Kuhn, C. and R. Weikard, *An investigation into the genetic background of coat colour dilution in a Charolais x German Holstein F2 resource population.* Anim Genet, 2007. **38**(2): p. 109-13.
61.   Schmutz, S.M. and D.L. Dreger, *Interaction of MC1R and PMEL alleles on solid coat colors in Highland cattle.* Anim Genet, 2013. **44**(1): p. 9-13.

62.	Brunberg, E., et al., *A missense mutation in PMEL17 is associated with the Silver coat color in the horse.* BMC Genet, 2006. **7**: p. 46.

63.	Clark, L.A., et al., *Retrotransposon insertion in SILV is responsible for merle patterning of the domestic dog.* Proc Natl Acad Sci U S A, 2006. **103**(5): p. 1376-81.

64.	Hellstrom, A.R., et al., *Inactivation of Pmel alters melanosome shape but has only a subtle effect on visible pigmentation.* PLoS Genet, 2011. **7**(9): p. e1002285.

65.	Kwon, B.S., et al., *Mouse silver mutation is caused by a single base insertion in the putative cytoplasmic domain of Pmel 17.* Nucleic Acids Research, 1995. **23**(1): p. 154-158.

66.	Kerje, S., et al., *The Dominant white, Dun and Smoky color variants in chicken are associated with insertion/deletion polymorphisms in the PMEL17 gene.* Genetics, 2004. **168**(3): p. 1507-18.

67.	Schonthaler, H.B., et al., *A mutation in the silver gene leads to defects in melanosome biogenesis and alterations in the visual system in the zebrafish mutant fading vision.* Dev Biol, 2005. **284**(2): p. 421-36.

68.	Andersson, L.S., et al., *Equine multiple congenital ocular anomalies and silver coat colour result from the pleiotropic effects of mutant PMEL.* PLoS One, 2013. **8**(9): p. e75639.

69.	Brumbaugh, J.A., *The ultrastructural effects of the I and S loci upon black-red melanin differentiation in the fowl.* Developmental Biology, 1971. **24**(3): p. 392-412.

70.	Burgoyne, T., et al., *Regulation of melanosome number, shape and movement in the zebrafish retinal pigment epithelium by OA1 and PMEL.* J Cell Sci, 2015. **128**(7): p. 1400-7.

71.	Kelsh, R.N., Brand, M., Jiang, Y.J., Heisenberg, C.P., Lin, S., Haffter, P., Odenthal, J., Mullins, M.C., van Eeden, F.J., Furutani-Seiki, M., Granato, M., Hammerschmidt, M., Kane, D.A., Warga, R.M., Beuchle, D., Vogelsang, L., and Nüsslein-Volhard, C., *Zebrafish pigmentation mutations and the processes of neural crest development.* Development, 1996. **123**: p. 369-389.

72.	Chakraborty, C., et al., *Zebrafish: A Complete Animal Model for In Vivo Drug Discovery and Development.* Current Drug Metabolism, 2009. **10**(2): p. 116-124.

73.	Lieschke, G.J. and P.D. Currie, *Animal models of human disease: zebrafish swim into view.* Nature Reviews Genetics, 2007. **8**(5): p. 353-367.

74.	Santoriello, C. and L.I. Zon, *Hooked! Modeling human disease in zebrafish.* Journal of Clinical Investigation, 2012. **122**(7): p. 2337-2343.

75.	Gestri, G., B.A. Link, and S.C. Neuhauss, *The visual system of zebrafish and its use to model human ocular diseases.* Dev Neurobiol, 2012. **72**(3): p. 302-27.

76.	Kari, G., U. Rodeck, and A.P. Dicker, *Zebrafish: an emerging model system for human disease and drug discovery.* Clin Pharmacol Ther, 2007. **82**(1): p. 70-80.

77.	Gross, J.M. and B.D. Perkins, *Zebrafish mutants as models for congenital ocular disorders in humans.* Mol Reprod Dev, 2008. **75**(3): p. 547-55.

78.	Bouhenni, R.A., et al., *Animal models of glaucoma.* J Biomed Biotechnol, 2012. **2012**: p. 692609.

79.	McMahon, C., E.V. Semina, and B.A. Link, *Using zebrafish to study the complex genetics of glaucoma.* Comparative Biochemistry and Physiology Part C: Toxicology & Pharmacology, 2004. **138**(3): p. 343-350.

80.   McGrath, P. and C.Q. Li, *Zebrafish: a predictive model for assessing drug-induced toxicity.* Drug Discov Today, 2008. **13**(9-10): p. 394-401.

81.   Parng, C., et al., *Zebrafish: A Preclinical Model for Drug Screening.* ASSAY and Drug Development Technologies, 2002. **1**(1): p. 41-48.

82.   Zhang, C., C. Willett, and T. Fremgen, *Zebrafish: an animal model for toxicological studies.* Curr Protoc Toxicol, 2003. **Chapter 1**: p. Unit1 7.

83.   Zon, L.I. and R.T. Peterson, *In vivo drug discovery in the zebrafish.* Nat Rev Drug Discov, 2005. **4**(1): p. 35-44.

84.   Stainier, D.Y.R., et al., *Guidelines for morpholino use in zebrafish.* PLoS Genet, 2017. **13**(10): p. e1007000.

85.   Taylor, J.S., et al., *Genome duplication, a trait shared by 22000 species of ray-finned fish.* Genome Res, 2003. **13**(3): p. 382-90.

86.   Richardson, R., et al., *The zebrafish eye-a paradigm for investigating human ocular genetics.* Eye (Lond), 2017. **31**(1): p. 68-86.

87.   McMahon, C., E.V. Semina, and B.A. Link, *Using zebrafish to study the complex genetics of glaucoma.* Comp Biochem Physiol C Toxicol Pharmacol, 2004. **138**(3): p. 343-50.

88.   Soules, K.A. and B.A. Link, *Morphogenesis of the anterior segment in the zebrafish eye.* BMC Dev Biol, 2005. **5**: p. 12.

89.   John, S.W.S., R.S.; Perkins, B.D.; Gray, M.P.; Savinova, O.V.; Dowling, J.E.; Link, B.A., *Characterization of the Zebrafish bug eye Mutation, Exploring a Genetic Model for Pressure-induced Retinal Cell Death.* Invest. Ophthalmol. Vis. Sci, 2003. **44S**: p. 1125.

90.   Link, B.A., et al., *Intraocular pressure in zebrafish: comparison of inbred strains and identification of a reduced melanin mutant with raised IOP.* Invest Ophthalmol Vis Sci, 2004. **45**(12): p. 4415-22.

91.   Gray, M.P., et al., *The aqueous humor outflow pathway of zebrafish.* Invest Ophthalmol Vis Sci, 2009. **50**(4): p. 1515-21.

92.   Chen, C.-C., et al., *Morphological Differences between the Trabecular Meshworks of Zebrafish and Mammals.* Current Eye Research, 2009. **33**(1): p. 59-72.

93.   Collery, R.F., et al., *Rapid, accurate, and non-invasive measurement of zebrafish axial length and other eye dimensions using SD-OCT allows longitudinal analysis of myopia and emmetropization.* PLoS One, 2014. **9**(10): p. e110699.

94.   Corey, D.R. and J.M. Abrams, *Morpholino antisense oligonucleotides: tools for investigating vertebrate development.* Genome Biology, 2001. **2**(5).

95.   Eisen, J.S. and J.C. Smith, *Controlling morpholino experiments: don't stop making antisense.* Development, 2008. **135**(10): p. 1735-43.

96.   Miller, J.C., et al., *An improved zinc-finger nuclease architecture for highly specific genome editing.* Nat Biotechnol, 2007. **25**(7): p. 778-85.

97.   Urnov, F.D., et al., *Genome editing with engineered zinc finger nucleases.* Nat Rev Genet, 2010. **11**(9): p. 636-46.

98.   Christian, M., et al., *Targeting DNA double-strand breaks with TAL effector nucleases.* Genetics, 2010. **186**(2): p. 757-61.

99.   Ran, F.A., et al., *Genome engineering using the CRISPR-Cas9 system.* Nat Protoc, 2013. **8**(11): p. 2281-2308.

100.   Doudna, J.A. and E. Charpentier, *Genome editing. The new frontier of genome engineering with CRISPR-Cas9.* Science, 2014. **346**(6213): p. 1258096.

101.   Varshney, G.K., et al., *High-throughput gene targeting and phenotyping in zebrafish using CRISPR/Cas9.* Genome Res, 2015. **25**(7): p. 1030-42.

102.   Zhang, F., Y. Wen, and X. Guo, *CRISPR/Cas9 for genome editing: progress, implications and challenges.* Human Molecular Genetics, 2014. **23**(R1): p. R40-R46.

103.   Deveau, H., J.E. Garneau, and S. Moineau, *CRISPR/Cas system and its role in phage-bacteria interactions.* Annu Rev Microbiol, 2010. **64**: p. 475-93.

104.   Horvath, P. and R. Barrangou, *CRISPR/Cas, the immune system of bacteria and archaea.* Science, 2010. **327**(5962): p. 167-70.

105.   Gasiunas, G., et al., *Cas9-crRNA ribonucleoprotein complex mediates specific DNA cleavage for adaptive immunity in bacteria.* Proceedings of the National Academy of Sciences, 2012. **109**(39): p. E2579-E2586.

106.   Cong, L., et al., *Multiplex genome engineering using CRISPR/Cas systems.* Science, 2013. **339**(6121): p. 819-23.

107.   Mali, P., et al., *RNA-guided human genome engineering via Cas9.* Science, 2013. **339**(6121): p. 823-6.

108.   Montague, T.G., et al., *CHOPCHOP: a CRISPR/Cas9 and TALEN web tool for genome editing.* Nucleic Acids Res, 2014. **42**(Web Server issue): p. W401-7.

109.   Gagnon, J.A., et al., *Efficient mutagenesis by Cas9 protein-mediated oligonucleotide insertion and large-scale assessment of single-guide RNAs.* PLoS One, 2014. **9**(5): p. e98186.

110.   Hu, J.H., et al., *Evolved Cas9 variants with broad PAM compatibility and high DNA specificity.* Nature, 2018. **556**(7699): p. 57-63.

111.   Kleinstiver, B.P., et al., *Engineered CRISPR-Cas9 nucleases with altered PAM specificities.* Nature, 2015. **523**(7561): p. 481-5.

112.   Hsu, P.D., E.S. Lander, and F. Zhang, *Development and applications of CRISPR-Cas9 for genome engineering.* Cell, 2014. **157**(6): p. 1262-78.

113.   Fu, Y., et al., *High-frequency off-target mutagenesis induced by CRISPR-Cas nucleases in human cells.* Nat Biotechnol, 2013. **31**(9): p. 822-6.

114.   Lin, Y., et al., *CRISPR/Cas9 systems have off-target activity with insertions or deletions between target DNA and guide RNA sequences.* Nucleic Acids Res, 2014. **42**(11): p. 7473-85.

115.   Tsai, S.Q., et al., *GUIDE-seq enables genome-wide profiling of off-target cleavage by CRISPR-Cas nucleases.* Nat Biotechnol, 2015. **33**(2): p. 187-197.

116.   Xie, S., et al., *sgRNAcas9: a software package for designing CRISPR sgRNA and evaluating potential off-target cleavage sites.* PLoS One, 2014. **9**(6): p. e100448.

117.   Doench, J.G., et al., *Optimized sgRNA design to maximize activity and minimize off-target effects of CRISPR-Cas9.* Nat Biotechnol, 2016. **34**(2): p. 184-191.

118.   Kleinstiver, B.P., et al., *High-fidelity CRISPR-Cas9 nucleases with no detectable genome-wide off-target effects.* Nature, 2016. **529**(7587): p. 490-5.

119.   Shen, B., et al., *Efficient genome modification by CRISPR-Cas9 nickase with minimal off-target effects.* Nat Methods, 2014. **11**(4): p. 399-402.

120.   Hruscha, A., et al., *Efficient CRISPR/Cas9 genome editing with low off-target effects in zebrafish.* Development, 2013. **140**(24): p. 4982-7.

121.   Hwang, W.Y., et al., *Efficient genome editing in zebrafish using a CRISPR-Cas system.* Nat Biotechnol, 2013. **31**(3): p. 227-9.

122. Irion, U., J. Krauss, and C. Nusslein-Volhard, *Precise and efficient genome editing in zebrafish using the CRISPR/Cas9 system.* Development, 2014. **141**(24): p. 4827-4830.

123. Hagerman, G.F., et al., *Rapid Recovery of Visual Function Associated with Blue Cone Ablation in Zebrafish.* PLoS One, 2016. **11**(11): p. e0166932.

124. Leighton, P.L.A., et al., *Prion gene paralogs are dispensable for early zebrafish development and have nonadditive roles in seizure susceptibility.* J Biol Chem, 2018. **293**(32): p. 12576-12592.

125. Noel, N.C.L. and W.T. Allison, *Connectivity of cone photoreceptor telodendria in the zebrafish retina.* J Comp Neurol, 2018. **526**(4): p. 609-625.

126. Huc-Brandt, S., et al., *Zebrafish prion protein PrP2 controls collective migration process during lateral line sensory system development.* PLoS One, 2014. **9**(12): p. e113331.

127. Meeker, N.D., et al., *Method for isolation of PCR-ready genomic DNA from zebrafish tissues.* Biotechniques, 2007. **43**(5): p. 610, 612, 614.

128. Bustin SA, B.V., Garson JA, Hellemans J, Huggett J, Kubista M, Mueller R, Nolan T, Pfaffl MW, Shipley GL, Vandesompele J, Wittwer CT., *The MIQE guidelines: minimum information for publication of quantitative real-time PCR experiments.* Clin Chem, 2009. **55**(4): p. 611-622.

129. Duval, M.G., A.P. Oel, and W.T. Allison, *gdf6a is required for cone photoreceptor subtype differentiation and for the actions of tbx2b in determining rod versus cone photoreceptor fate.* PLoS One, 2014. **9**(3): p. e92991.

130. Chang, Y.-F., J.S. Imam, and M.F. Wilkinson, *The Nonsense-Mediated Decay RNA Surveillance Pathway.* Annual Review of Biochemistry, 2007. **76**(1): p. 51-74.

131. Hug, N., D. Longman, and J.F. Caceres, *Mechanism and regulation of the nonsense-mediated decay pathway.* Nucleic Acids Res, 2016. **44**(4): p. 1483-95.

132. Kurosaki, T. and L.E. Maquat, *Nonsense-mediated mRNA decay in humans at a glance.* J Cell Sci, 2016. **129**(3): p. 461-7.

133. Cechmanek, P.B. and S. McFarlane, *Retinal pigment epithelium expansion around the neural retina occurs in two separate phases with distinct mechanisms.* Dev Dyn, 2017. **246**(8): p. 598-609.

134. Greenhill, E.R., et al., *An iterative genetic and dynamical modelling approach identifies novel features of the gene regulatory network underlying melanocyte development.* PLoS Genet, 2011. **7**(9): p. e1002265.

135. Seberg, H.E., et al., *TFAP2 paralogs regulate melanocyte differentiation in parallel with MITF.* PLoS Genet, 2017. **13**(3): p. e1006636.

136. Thisse, B., Pflumio, S., Fürthauer, M., Loppin, B., Heyer, V., Degrave, A., Woehl, R., Lux, A., Steffan, T., Charbonnier, X.Q. and Thisse, C., *Expression of the zebrafish genome during embryogenesis.* 2001.